Constraining the Opening of the Red Sea: Evidence from the Neoproterozoic Margins and Cenozoic Magmatism for a Volcanic Rifted Margin

Robert J. Stern and Peter R. Johnson

Abstract

As the Earth's best-known example of an active, incipient ocean basin, the Red Sea provides crucial information about continental rifting and the tectonic transition from extended continental crust to seafloor spreading. Study of the Red Sea over the past decades has given many answers, but significant questions remain about how and when it opened because of lacking or ambiguous data and thick salt cover. A key issue is the geometry of the pre-rift join between the Arabian and Nubian Shields that form the basement flanking the Red Sea because this constrains the nature of Red Sea crust. The Neoproterozoic basement rocks flanking the Red Sea contain prominent shears and sutures between amalgamated tectonostratigraphic terranes, regions of transpressional shortening, and brittle-ductile faults related to Ediacaran orogenic collapse and tectonic escape. These structures vary in orientation from orthogonal to oblique with respect to the Red Sea coastlines. Importantly, they correlate across the Red Sea, and provide piercing points for a near coast-to-coast palinspastic reconstruction of the Arabian and Nubian Plates along the entire Red Sea. A tight pre-rift fit of the Arabian and Nubian Shields implies that most of the Red Sea is underlain by oceanic crust. Potential-field data are compelling evidence for oceanic crust along the axis of the Red Sea south of latitude ~22°N, persuasive for the margins of the southern Red Sea, and suggestive for the northern Red Sea. A variety of 20–24 Ma dikes, gabbros, and basaltic flows emplaced during the early stages of Red Sea rifting are consistent with Miocene asthenospheric upwelling, partial melting, and intrusion that would have weakened and facilitated rupture of the ~40-km thick continental crust and thicker mantle lithosphere of the then contiguous Arabian and Nubian Shields. The dikes, gabbros, and basaltic flows emplaced during the early stages of Red Sea rifting are strong evidence furthermore that the Red Sea is an example of a volcanic-rifted margin. Offshore seismic profiling designed to image beneath the salt followed by drilling to basement in the Red Sea are required to test these ideas.

1 Introduction

The Red Sea is a ~300 km wide nascent ocean centred on a well-defined active divergent boundary between the formerly continuous Neoproterozoic rocks of the Arabian Shield and Nubian Shield (ANS) (Fig. 1) that are now parts of the Arabian and Nubian (or African) plates. The Red Sea is Earth's best example of an active, incipient ocean basin that has progressed from continental rifting to seafloor spreading (Bonatti et al. 2015; Bosworth 2015). It is therefore an important natural laboratory in which to test rift-to-drift models of continental rifting and to refine our understanding of the nature of the crust beneath continent-ocean transitions and the formation of passive continental margins. However, although the Red Sea has been studied by geologists, geomorphologists, and geophysicists for more than six decades, so that much is known about the region, many aspects of Red Sea development are unresolved because of geological and logistical problems. Geologic problems include the effect of a thick sediment cover (including salt) that prevents direct observation of most Red Sea crust (Orszag-Sperber et al. 1998); logistical problems for integrated study stem from the Red Sea geographic spread across the jurisdiction of six nations, and the differing approaches and objectives of industrial and academic researchers and terrestrial and marine geoscientists. Most data for models of Red Sea development come from the Gulf of Suez, and the margins of Egypt and Yemen, whereas the rift flanks of Saudi Arabia and Sudan are understudied leaving a large information gap along the central portions of the Red Sea (Szymanski et al. 2007).

R. J. Stern (✉)
Geosciences Department, University of Texas at Dallas, Richardson, TX 75080-0688, USA
e-mail: rjstern@utdallas.edu; bobdadbob@yahoo.com

P. R. Johnson
6016 Haines Street, Portland, OR 97219, USA

N. M. A. Rasul and I. C. F. Stewart (eds.), *Geological Setting, Palaeoenvironment and Archaeology of the Red Sea*,
https://doi.org/10.1007/978-3-319-99408-6_4

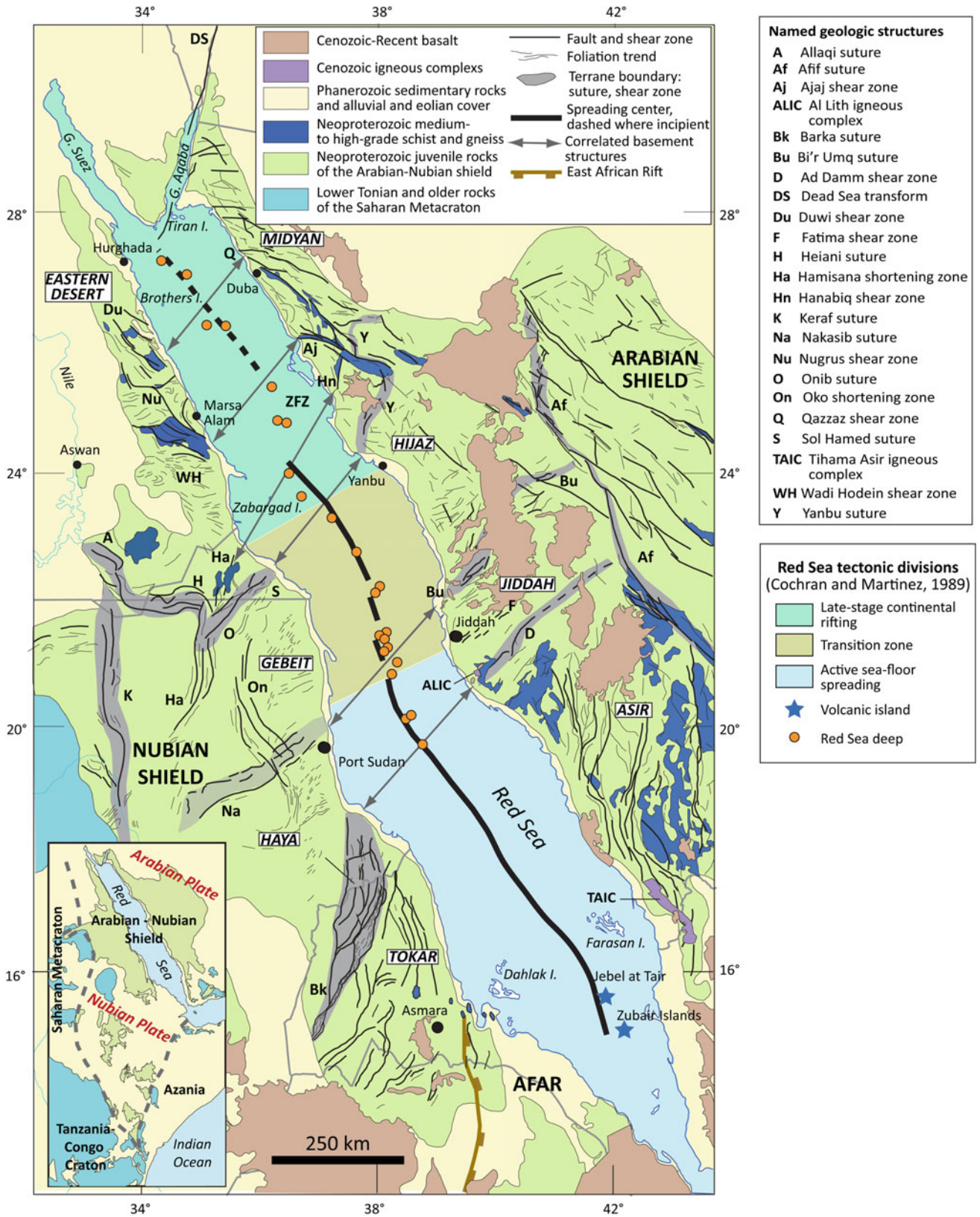

Fig. 1 Major geologic features of the Red Sea (spreading ridges, deeps), surrounding uplifted margins of the Arabian and Nubian Shield (ANS), and distribution of Late Cenozoic lava fields or harrats. These harrats bring fragments of the ANS lower crust and upper mantle to the surface as mafic and ultramafic xenoliths

Nonetheless, an extensive literature about the Red Sea is now available, including the series of papers about Red Sea research between 1970 and 1975 published by the Saudi Arabian Directorate General of Mineral Resources (DGMR 1977) and the recent collection of papers resulting from a 2013 workshop on Red Sea geology, geography, and biology sponsored by the Saudi Geological Survey (Rasul and Stewart 2015). As a consequence, many aspects of Red Sea development are well established; others, however, continue to be debated.

Here we consider two related issues: (1) the geometry of the pre-rift join between the Arabian and Nubian Plates, and (2) the nature of the crust beneath the Red Sea. We do this by reviewing what we know about the nature of Red Sea crust and the magmatic history of the Red Sea basin; by identifying structures in the Neoproterozoic rocks of the ANS that correlate across the Red Sea and provide "piercing-points" for the palinspastic reconstruction of the Arabian and Nubian Plates; and by considering the composition and vertical structure of ANS lithosphere as factors that should affect the strength of the lithosphere and thus how it ruptures. We use this review to argue for a near coast-to-coast palinspastic reconstruction of the Arabian and Nubian Plates, to propose that oceanic crust underlies more of the Red Sea than is generally considered, and to propose a volcanic-rifted margin (VRM) origin for the Red Sea in the light of VRM models used to account for continental-oceanic rifting elsewhere.

A large proprietary geophysical, stratigraphic, and lithologic dataset is held by petroleum exploration companies working on either side of the Red Sea. However, the results are not available for consideration here, and our review is based on published geologic maps and reports, publicly available geophysical information, and journal articles. Consequently, conclusions made here are limited by the level of detail in these sources and, as with all things pertaining to the structure of the Red Sea, would benefit immeasurably from future drilling and geophysical surveys. We are also aware of the difficulty of making pre-Red Sea-spreading reconstructions, as discussed by Coleman (1993), because of assumptions made about the structure of plate boundaries. Kinematic models proposed for the plate motions within the Red Sea area during the last 4–5 million years have met with some success. This is because it is reasonable to assume instantaneous motions of plates with rigid plate boundaries about Euler poles of rotation. However, Coleman (1993) argues that pre-5 Ma reconstruction are problematic because plate boundaries were probably more diffuse as a result of modification to the Red Sea basement prior to the onset of sea-floor spreading by normal faulting, thinning, and mafic intrusion and underplating. Geodetic (GPS), plate tectonic, and geologic observations indicate that the present rate of extension across the Red Sea is 24 ± 1 mm/y in the south and 7 ± 1 mm/y in the north (Reilinger et al. 2015). This rate probably pertained since ~11 Ma, whereas the extension rate prior to that was about half. Recognizing a clear distinction between the onset of rifting and the onset of sea-floor spreading, Coleman (1993) points out that the Gulf of Suez is an example of early extension within the rift zone and that the southern Red Sea underwent considerable extension without the production of oceanic crust. Nonetheless, we are impressed by the overall pattern that emerges from correlating flanking Neoproterozoic structures to argue for a relatively tight pre-Red Sea-spreading juxtaposition of plates. This implies a different history for Red Sea basin evolution than is commonly generally accepted (e.g., Cochran 1983; Bosworth 2015).

2 Red Sea Overview

As recognized by Wegener (1920), the Red Sea is the result of rupture of continental crust and transition into an oceanic basin that has occurred in a complex system of continental extension represented by the Gulf of Aden, East African, and Red Sea rifts. The rifts meet at a triple junction in the Afar region of Eritrea, Djibouti, and Ethiopia, but individually show different stages of development (Bonatti et al. 2015). In this paper, the term "Red Sea" refers to the region covered by present-day seawater, whereas "Red Sea basin" refers to the wider structure comprising the present-day sea and its oceanic crust, Mesozoic-Cenozoic sedimentary rocks deposited on the shelves and coastal plain along the margins of the Red Sea, and coeval Mesozoic-Cenozoic sedimentary rocks preserved in fault basins that reflect pervasive extension across a broader region inland from the Red Sea.

The Red Sea itself is 1900 km long and a maximum of 355 km wide. South of latitude ~21°N (Fig. 1), it has an axial trough 1000–2900 m deep and shallow marine shelves <50 m deep. Between ~21° and 25°N, the bathymetric trough is discontinuous and the axial part of the Red Sea forms a series of deeps that contain basaltic cones, dense, hot brines and deposits of Fe, Cu, and Zn (Schardt 2016). North of latitude 25°N, the Red Sea has a common depth of 1200 m; it is punctuated by deeps but lacks an axial trough. The southern marine shelves and most of the northern Red Sea are underlain by sedimentary rocks that include pre-rift Late Cretaceous to Early Oligocene sandstone, shale and carbonates; syn-rift Early to Middle Miocene Globigerina marl, carbonate, and sandstone; and kilometre-thick sequences of late-rift Middle Miocene to Recent anhydrite, halite, shale, and sandstone (Bosworth 2015).

Although some authors see the Cretaceous-Paleogene embayment that extended south from Tethys Ocean toward Jiddah subparallel to the present day Red Sea axis as a harbinger of the eventual Red Sea rift (d'Almeida 2010), the onset of extension in the Red Sea region is generally

considered to be early Miocene, marked by the beginning of deposition of syn-rift sediments (see review by Bosworth 2015). Several stages in development of the overall Gulf of Aden-Red Sea rift system are recognized (Bosworth 2015), including: (1) plume-related basaltic and rhyolitic volcanism at ~31 Ma in the Afar region and SW Yemen that subsequently spread northward into western Saudi Arabia; (2) deposition of marine, syntectonic sedimentary rocks in the central Gulf of Aden between ~29.9 and 28.7 Ma, followed by Early Oligocene rifting in the Gulf of Aden; (3) formation of a small rift basin in the Eritrean Red Sea between ~27.5 and 23.8 Ma, virtually concurrent (~25 Ma) with extension and rifting in the Afar; (4) intrusion of layered gabbro, granophyre, and basaltic dike swarms in southern Arabia at ~24–23 Ma, eruption of early syn-rift basaltic flows (harrats) in southern and northwestern Arabia and in the subsurface in the Cairo region of Egypt, emplacement of basaltic dikes along the margin of, what is now, western Arabia, rift-normal extension, rift-margin uplift (Szymanski 2013), and a deepening of the Red Sea basin marked by a transition to predominantly Globigerina-rich marl and deepwater limestone (Bosworth et al. 2005); (5) penetration of the Dead Sea transform into the continental crust of the northern Arabian Plate at ~14–12 Ma and cessation of rifting in the Gulf of Suez; (6) from ~10 Ma onward, eruption of a younger phase of Oligocene-Recent syn-rift basaltic lava forming the lava fields (harrats) of the western and northern Arabian Plate; and (7) onset of oceanic accretion by ~5 Ma, if not earlier, and the development of organized spreading in the southern Red Sea and, to a debated extent, in the northern Red Sea. As noted by Bosworth et al. (2005), initiation of continental extension marked by the intrusion of mafic dikes and normal faulting, was virtually instantaneous between Eritrea, Egypt, and northwestern Arabia, at the Oligocene-Miocene transition. Extension was initially orthogonal to the trend of the Red Sea, but by 14 Ma, at the time of initiation of the Dead Sea transform, extension became oblique to the Red Sea.

The crux of the debate about Red Sea development hinges on the interpretation of south-to-north morphologic and geophysical variations as approximating a tectonic evolutionary sequence from drifting in the south to rifting in the north (Cochran 1983). The southern axial trough and magnetic anomalies are treated as evidence of active seafloor spreading. In the north, the absence of an axial trough and Vine-Matthews magnetic anomalies and the presence of extensive syn-rift sedimentary rocks are interpreted as evidence that the Red Sea here is a continental rift, which has developed nearly to the point of seafloor spreading (Martinez and Cochran 1988; Lazar et al. 2012; Ligi et al. 2012). Bosworth (2015) concluded that this crust may be highly extended continental material or mixed continental and volcanic material. The central part of the Red Sea between about 21°N and 23°N is regarded as a transitional zone between oceanic and continental rifting (Cochran and Martinez 1988) (Fig. 1) in which the cluster of prominent deeps is interpreted as isolated spreading cells above 'hot points' where upwelling mantle diapirs puncture continental lithosphere (e.g., Bonatti 1985; Bonatti et al. 2015). The Gulf of Suez at the northern end of the Red Sea is an entirely continental rift formed by a complex half graben broken along strike into a series of smaller half grabens. Each half graben consists of nested rotated fault blocks that displace both sedimentary fill and crystalline continental basement (Bosworth 2015). Because its structure is so well known as a result of excellent exposure and a vast amount of drilling and geophysical surveying, the Gulf of Suez is commonly used as a model for the northern Red Sea, although the much deeper seafloor of the northernmost Red Sea requires a different crustal structure.

The widely accepted timing of initial seafloor spreading at ~5 Ma is based on interpreting the age of large-amplitude, short wavelength magnetic anomalies centred on the axial trough of the Red Sea between latitudes ~23.5°N and 15°N. A limited section of these anomalies is shown in Fig. 2a; they are more fully shown in a residual magnetic anomaly map of the Red Sea compiled by Hall et al. (1977). The anomalies trend NW parallel to the Red Sea and are interpreted as Vine-Matthews type magnetic anomalies indicative of newly formed oceanic crust (Girdler and Styles 1974; Roeser 1975; Hall et al. 1977). By comparison with worldwide magnetostratigraphy, the oldest anomalies are estimated to be 5 Ma, the youngest 0 Ma. As shown in Fig. 2a, the linear magnetic anomalies in the axial region of the southern Red Sea are flanked by broader, lower amplitude anomalies that extend as far as the coastlines and even onto part of the coastal plain. The nature of these anomalies is debated, but Girdler and Styles (1974), Hall (1989), and Hall et al. (1977) interpret them as also caused by oceanic crust, although older than the crust in the axial region and reduced in amplitude because of the 4–5 km sedimentary sequence covering them (Rasul et al. 2015). These anomalies are estimated to be either 25–26 Ma or 35–37 Ma, and on this basis two stages of Red Sea sea-floor spreading are proposed (Girdler and Styles 1974). The first stage spanned 41–34 Ma and the second stage occurred from 4–5 Ma to the Present. The southern Red Sea axial trough is further marked by a continuous gravity high (Fig. 2B) and high heat flow, consistent with the emplacement of oceanic crust. Between ~21° and 25°N, where the bathymetric trough is discontinuous, large-amplitude magnetic anomalies are associated with the deeps and basaltic intrusions. North of latitude 25°N, the Red Sea has neither trough nor obvious spreading-related linear magnetic anomalies and the ocean crust is largely considered to be extended continental material analogous to the Gulf of Suez. However, combined

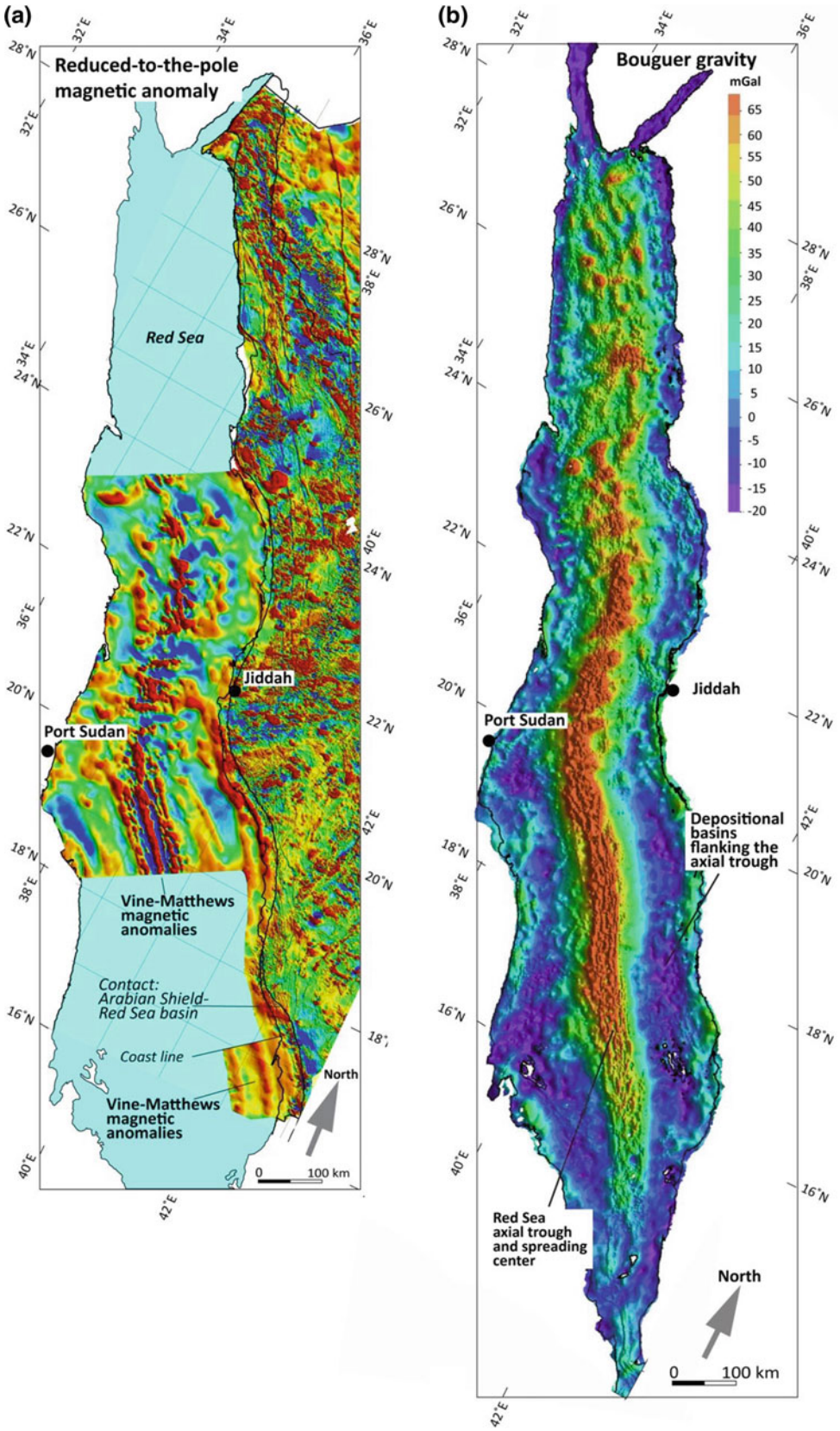

Fig. 2 Potential-field data for the Red Sea. **a** Reduced-to-the-pole magnetic anomaly map for the central Red Sea surveyed in 1976 (after Zahran et al. 2003). The plot uses the conventional color scheme of red for high intensity and blue for low intensity. The image shows magnetic stripes composed of narrow magnetic highs and lows along the Red Sea axial trough and its eastern margin south of 20°N corresponding to Vine-Matthews-type anomalies indicative of seafloor spreading. Discontinuous highs and lows north of 20°N reflect the transition zone of seafloor spreading shown in Fig. 1. **b** Bouguer gravity of the Red Sea generated from TOPEX/Poseidon satellite data (cf., Stewart and Johnson 1994) and presented at a 1-km grid interval. The image shows a virtually continuous gravity high extending from 16°N to 24°N coincident with the axial trough. The gravity high is consistent with the emplacement of mafic material, and suggests active ocean floor spreading at least as far north as 24°N

3-D interpretations of gravity and aeromagnetic data suggest a different crustal structure. Beneath the northern Red Sea, hot upper mantle is present from within a few tens of kilometres of the coastlines and the crust thins from 21 km at the Egyptian coast to 8–12 km thick (excluding the thick sediments) offshore (Saleh et al. 2006).

At the surface, the boundary between the Red Sea basin and the flanking Arabian-Nubian Shield is a depositional-to-faulted contact between sedimentary and locally volcanic rocks of the basin and Neoproterozoic basement rocks. The boundary is reasonably clear in outcrop despite cover by Recent alluvium and colluvium, and well defined in potential-field (magnetic and gravity) (Fig. 2) and seismic-refraction surveys (Fig. 3). A seismic reflection survey of the seaward portion of the coastal plain in southwest Saudi Arabia made in the 1960s (Gillman 1968) indicated that the surface of the Jurassic/basement contact dipped toward the Red Sea at about 10°, deepening from about 2 km deep 20 km inland to nearly 5 km at the coastline near the Mansiyah No. 1 drill hole and the Jizan salt dome (for locations, see Fig. 7). Unfortunately, the Mansiyah drill hole had to be abandoned at 3.9 km depth, short of seismic basement. The reflection survey profiles did not extend northeastward onto the Neoproterozoic basement of the Arabian Shield, and therefore its seismic properties could not be compared with those of basement beneath the coastal plain. This same locality was covered by the 1978 Riyadh-Farasan seismic-refraction survey conducted by the Saudi Arabian Deputy Ministry for Mineral Resources and the U.S. Geological Survey Saudi Arabian Mission (Mooney et al. 1985) (Figs. 3 and 7) which shows an abrupt thinning of continental crust from ~40 km beneath the Arabian Shield to ~20 km beneath the coastal plain and ~10 km beneath the Farasan Islands coincident with an inferred transition from continental to oceanic crust (Mooney et al. 1985; Gettings et al. 1986). The seismically indicated transitional crust is characterized by P-wave velocities between 6 and 8 km/s, and is interpreted by Blank et al. (1986) as oceanic crust produced during early stages of seafloor spreading and strong evidence in support for a hypothesis of essentially shore-to-shore opening in this part of the Red Sea. A recently published study of teleseismic P-wave receiver functions in Egypt (Hosny and Nyblade 2016) indicates thinning of continental crust from 35–39 km inland to 30 km at the northern Red Sea coast. There are no results for the crustal thickness of the Red Sea itself although a figure in the Hosny and Nyblade paper suggests crustal thicknesses of <20 km offshore, but the model illustrated is not precise enough to make any conclusion about the nature of crust beneath the northern Red Sea.

The contact between the ANS basement and the Red Sea basin is generally exposed within 25 km of the shoreline, and the relatively narrow coastal plain between the ANS and the Red Sea coast is underlain by Neogene sedimentary and minor volcanic rocks. In places, however, abrupt changes in the strike of the contact and the development of embayments and fault basins shift the contact more than 100 km inland, testifying to tectonic complexity. The Lisan basin at ~28°N in NW Saudi Arabia, for example, is a broad region of Cenozoic sedimentary rocks and ANS basement horsts in a structurally complex region where the Gulf of Suez, Dead Sea Transform, and Red Sea meet (Fig. 4). Drag along the Dead Sea Transform caused folding and anticlockwise rotation of Cenozoic rocks in the Lisan basin and a 110 km-sinistral slip of the basin rocks from their original position contiguous with the Gulf of Suez. The Gulf of Aqaba remains the most active seismic area in Saudi Arabia and is the site of the last two (1983 and 1995) major earthquakes (Roobol and Stewart 2009).

Other embayments include the Nakheil basin at ~26°N in Egypt (Khalil and McClay 2002; Abd el-Wahed et al. 2010) and Azlam (Aznam) basin at about ~27°N in Saudi

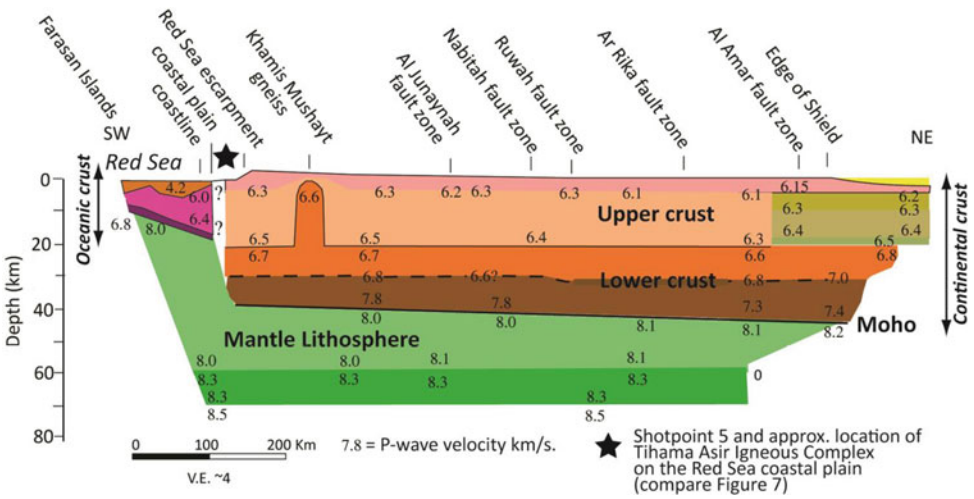

Fig. 3 Interpretive section showing crustal structure based on P-wave velocities (km/s) along the 1978 Riyad-Farasan seismic-refraction profile that extends southwesterly from central Saudi Arabia to the Farasan Islands in the Red Sea (after Mooney et al. 1985)

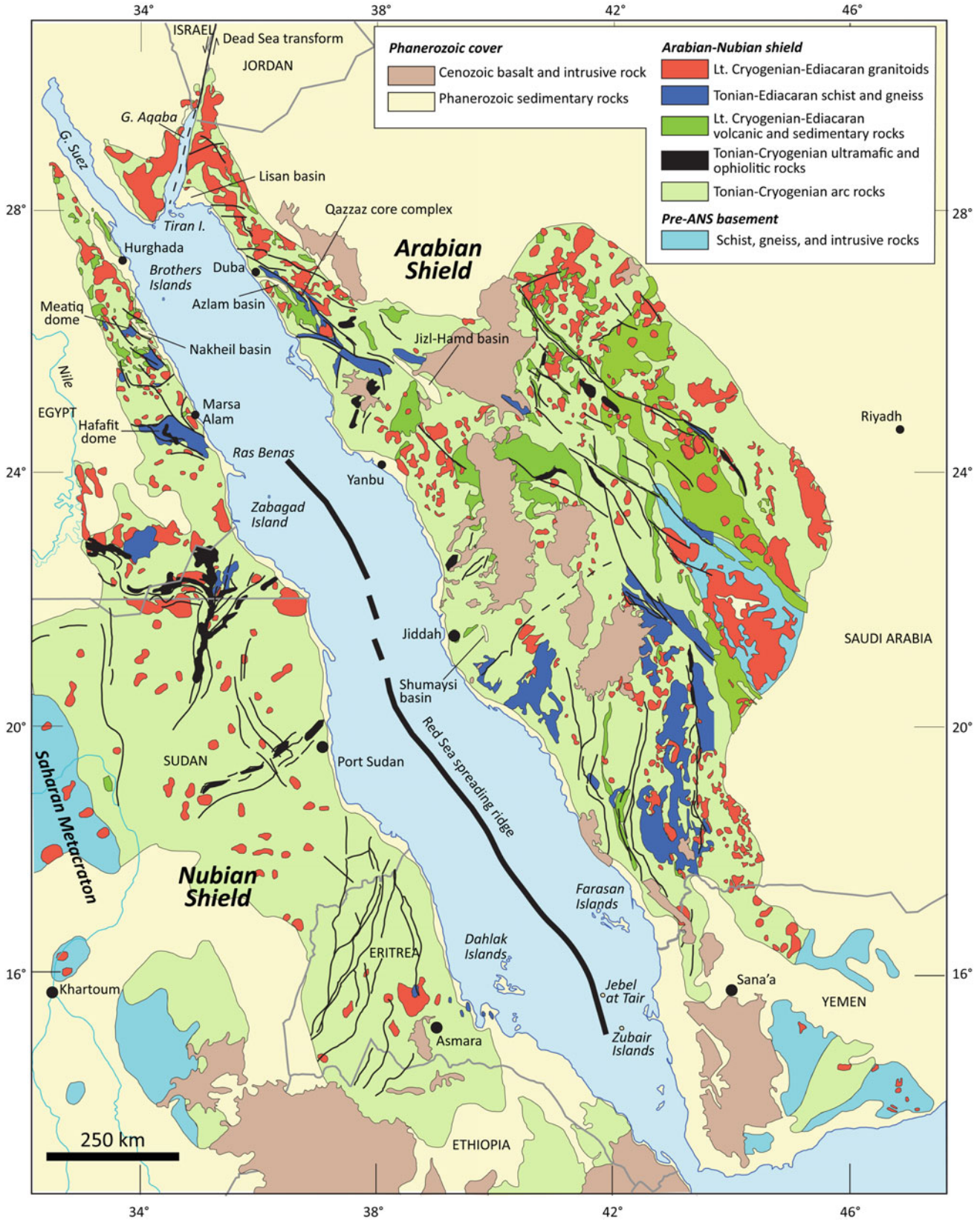

Fig. 4 Simplified geologic map of the Arabian-Nubian Shield

Arabia (Suayah et al. 1991) (Fig. 4). These basins are filled by pre- and syn-rift Mesozoic-Cenozoic sedimentary rocks, and extend into the basement oblique to the general trend of the Red Sea as extensional structures focused along reactivated, preexisting NW-trending Neoproterozoic Najd shear zones. They may have been originally one continuous basin. The Shumaysi basin (E of Jiddah) and the Jizl-Hamd basin (north of Yanbu) are fault basins isolated from the Red Sea by intervening blocks of Neoproterozoic rocks. Apatite and zircon (U-Th)/He thermochronology identifies a prolonged period of diffuse extension associated with the development of these basins, particularly an ~8 million-year period of block faulting that created a ~200 km-wide zone of diffuse extension associated with the Jizl-Hamd half graben (Szymanski 2013; Szymanski et al. 2012, 2016).

The Gulf of Suez at the northern end of the Red Sea lacks evidence of volcanic rocks, intrusive rocks, or sea-floor spreading and is a region of well-defined normal faulting and thinned continental crust (Khalil and McClay 2001; Bosworth 2015). The abrupt change in depth from a few metres below sea level in the southern Gulf of Suez to >1200 m in the northern Red Sea suggests an abrupt change in crustal type at the transition between the Gulf and the Red Sea. The Gulf of Aqaba, which marks the southern extension of the Dead Sea transform, is a narrow, transtensional basin with seafloor down to 1850 m deep. This active plate boundary has faulting and earthquakes but no known igneous activity.

ANS crust is exposed on Tiran Island at the northern end of the Red Sea (Goldberg and Beyth 1991) and is present farther south as Neoproterozoic granitic gneiss and peridotite in a horst of continental crust extending SSE from Ras Benas in Egypt to Zabargad Island (Brueckner et al. 1996). Granitic rocks are encountered elsewhere as much as 20 km from the Egyptian and Saudi Arabian coastlines (Bosworth et al. 2005). Other islands in the Red Sea, however, are underlain by Cenozoic to Recent reef material, such as the Farasan and Dahlak Islands, or by Recent volcanic rock, such as Jebel at Tare and Zubeir Islands (Fig. 4).

It is well known that young rifted continental margins are flanked by large-scale, low-relief plateaux elevated 1 to 2 km or more above sea level as the result of rift-margin uplift or post-rift exhumation and uplift (Japsen et al. 2011). Such uplifted margins may remain exposed for some tens of millions of years after the onset of seafloor spreading, as is the case of crystalline rocks exposed in Norway and Greenland on the flanks of the North Atlantic Ocean, which began seafloor spreading ~54 Ma (Gaina et al. 2009). As the opening ocean matures and widens, the uplifted rift flanks subside and are buried with sediments to become complementary passive continental margins, such as the flanks of the Central Atlantic and Gulf of Mexico, where seafloor spreading began >150 Ma. In these cases, only the largest, most regional basement features can be correlated across the ocean basin, and only broad inferences can be made about the possible effects of basement structures on ocean opening and oceanic crustal composition. In the case of the Red Sea however, rift-margin uplift was recent enough that the basement rocks persist as prominent rift-flank uplifts on either side of the Red Sea, and excellent exposures in these uplifts allow relatively straightforward correlation of basement structures across the Red Sea ("piercing-points").

North-to-south morphologic differences, nevertheless, characterize the dynamic topography resulting from Red Sea rift-flank uplift, mimicking changes seen in the Red Sea itself. Low-temperature (U-Th)/He thermochronology shows that the west-central Saudi Arabian Red Sea margin in an area referred to as the central Arabian rift flank (CARF) was partly exhumed at ~350 Ma but for much of the subsequent Mesozoic was relatively stable (Szymanski 2013; Szymanski et al. 2012, and in prep.). However, a complex Middle Miocene cooling history shows that the onset of Red Sea rifting was associated with footwall exhumation at ~23 Ma during which the CARF was dissected along rift-parallel fault blocks and exhumed from pre-rift flank depths of ~1.5–3.9 km (Szymanski et al. 2012, and in prep.). A comparable exhumation signal elsewhere along the Red Sea Nubian margin and the southern Arabian rift flank in Saudi Arabia and Yemen indicates that Red Sea rifting began along nearly the entire length of the Red Sea-Gulf of Suez system at ~23 Ma (Szymanski et al. 2012, and in prep.). A formerly extensive cover of Phanerozoic sedimentary rocks was stripped off the Arabian-Nubian Shield around the Red Sea but remnants are preserved as outliers unconformable on basement rocks at the top of the Red Sea escarpment and in blocks on the Red Sea coastal plain down-faulted along a W-dipping detachment that formed during Red Sea extension (Bohannon 1989). Rift margins in the south rise in erosional escarpments to elevations of more than ~3000 m. In Arabia, the escarpment is a continuous topographic feature south of Jiddah and the lip of the escarpment is the watershed between drainages to the Red Sea and to the Persian/Arabian Gulf. North of the Jiddah area, in contrast, the escarpment is discontinuous and is no longer a watershed. Drainage from far inland cuts through the mountains inland from the Red Sea in contrast to the sharp drainage divide present in the south. A similar topography occurs west of the Red Sea, with a prominent escarpment flanking the coastal plain in Eritrea and southern Sudan, but only mountains and valleys, not a continuous escarpment, in northern Sudan and Egypt. This suggests that the southern Red Sea rift flanks have been recently rejuvenated but that the northern margins have not.

3 The Red Sea Basin as a Magmatic Province

In addition to its dynamic rift-related topography, development of the Red Sea was accompanied by the emplacement of abundant dikes, sills, and volcanic flows (Bosworth and Stockli 2016) (Fig. 5).

Overall, Red Sea magmatism is decidedly asymmetric, with a preponderance of dike emplacement and basalt eruptions along the western margin of the Arabian Plate (Fig. 5). The earliest magmatism in the region was related to the Afar plume in the form of pre-rift mafic lavas extruded in Ethiopia, Eritrea, and southern Yemen at ~31 Ma. The earliest rift-related Red Sea magmatism comprised swarms of syn-rift mafic tholeiitic dikes, gabbroic intrusions, and volcanic rocks emplaced between ~24 and 20 Ma, and extending over 3000 km from north of Afar into northern Egypt (Bosworth and Stockli 2016) and northern Jordan-southern Syria (Harrat ash Shaam) (Ilani et al. 2001). Particular concentrations of dikes and intrusions make up the Al Lith igneous complex (ALIC) 100 km SE of Jiddah (Figs. 1 and 6) and the Tihama Asir igneous complex (TAIC) 40–100 km east and north of Jizan (Figs. 1 and 7). The dikes formed from magmas produced by partial melting of the mantle (Coleman 1993) and make up swarms of sheeted sequences, as in the igneous complexes, or wide and elongate dikes forming extensive linear structures. The latter do not crop out everywhere but are indicated along most of the Red Sea eastern margin by narrow magnetic lineaments such as those on the RTP aeromagnetic anomaly map of western Saudi Arabia in Fig. 2a. North of latitude 22°N, the magnetic lineaments are virtually continuous, indicating that the dikes extend tens to hundreds of kilometres along strike; south of 22°N, the dikes are less continuous. They yield $^{40}Ar/^{39}Ar$ ages of ~21 Ma (Sebai et al. 1991). Contemporaneous dikes and lava flows (23–22 Ma) mapped in the subsurface in the Cairo area possibly originated from a short-lived "mini-plume" (Bosworth 2015; Bosworth and Stockli 2016).

Following a ~7–9 million-year quiescence, apart from local volcanism in the Afar area and at Harrats Ishara (~17–14.5 Ma; Szymanski 2013) and Harairah between Madinah and Al Wajh (Fig. 5), Middle Miocene resumption of magmatism in the Red Sea basin resulted in new basaltic flows at Harrat ash Shaam (<~13 Ma) and formed the younger harrats of Saudi Arabia (Nawasif/Al Buqum, Kishb, Rahat, Khaybar and Ithnayn, and Uwayrid). Ilani et al. (2001) envisage that this renewal of volcanism was associated with sinistral movement along the Dead Sea transform, and may reflect the emergence of upper-mantle upwelling beneath the western Arabian Plate. Recent volcanic and dike activity is evidenced at Harrats Rahat and Lunayyir in the past 800 years until the Present (Pallister et al. 2010) in northwestern Saudi Arabia and on the coastal plain east of Jizan. As pointed out by Bosworth and Stockli (2016), Red Sea magmatism was episodic and although it gave rise to the prominent fields of basalt that characterize the western Arabian Plate, the exposed erupted and intruded magmatic material does not amount to a large volume when considered in relation to other rifted margins. Nevertheless, the presence of the sheeted dikes and plutons of the Al Lith and Asir Tihama complexes show that oceanic-like rifting, albeit briefly, accompanied the early phase of the Red Sea rift history (Bosworth and Stockli 2016). Furthermore if, as contended in this paper, more of the Red Sea is underlain by oceanic material than conventionally accepted, the overall volume of magmatic material is considerable.

The Al Lith Igneous Complex comprises two sets of dikes and small gabbro and diorite plutons that intrude crystalline rocks of the Arabian Shield (Fig. 6) and volcanic rocks that interdigitate with other epiclastic rocks of the Red Sea basin (Pallister 1987). The volcanic rocks (Sita Formation) are a suite of basalt, dacite, and rhyolite interbedded with volcaniclastic rocks, wacke, and limestone. One set of dikes, referred to as the Ghumayqah complex, consists of widely spaced linear intrusions of gabbro to monzogabbro 10–100 m wide. The Ghumayqah dikes create prominent magnetic anomalies (Fig. 6b). The anomalies and geologic mapping show that two NW-trending dikes shown in Fig. 6a extend more than 50 km SE of the area shown in the figure where they are associated with as many as ten, widely spaced, similar dikes intruded into basement across a width of ~30 km (Pallister 1986). The other set of dikes, referred to as the Damm dike complex, forms swarms of subparallel to parallel, and locally sheeted, dikes and minor sills of alkali basalt and lesser hawaiite, trachyte, comendite, dacite, and rhyolite. This swarm extends over a width of 10 km. Because of greenschist-facies metamorphism, K-Ar dating reported by Pallister (1987) is not as reliable as the $^{40}Ar/^{39}Ar$ dating reported by Sebai et al. (1991). Whole-rock plateau ages range from 26.0 ± 1.3 Ma to 22.3 ± 0.5 Ma and amphibole ages range from 24.0 ± 0.2 Ma to 22.3 ± 0.6 Ma (Sebai et al. 1991). Pallister (1987) interprets the Al Lith Igneous Complex as magmatism in continental crust thinned and extended by horst-graben faulting, and envisages a sheeted mafic dike complex forming the Red Sea oceanic crust farther west (Fig. 6c). The conspicuous magnetic boundary shown on Fig. 6b and regionally shown on Fig. 2a is located where SW-trending anomalies reflecting the structure of the Arabian Shield are truncated by a regional high that extends along the entire eastern margin of the Red Sea south of Jiddah, and is interpreted by us as the boundary between continental and oceanic crust.

The Tihama Asir igneous complex (Fig. 7) comprises swarms of sheeted dikes, bodies of layered gabbro, and

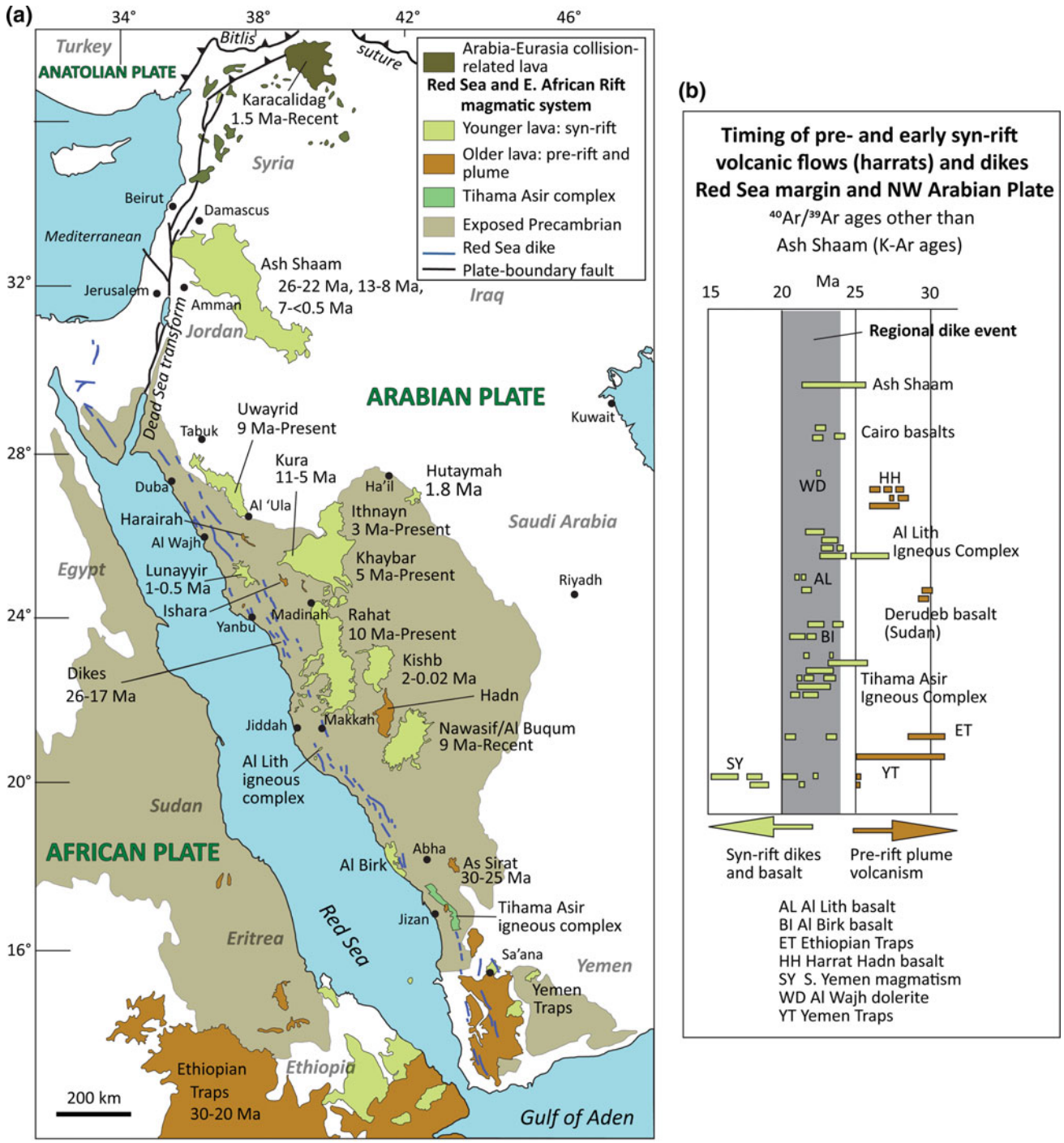

Fig. 5 **a** Cenozoic to Recent volcanic and intrusive rocks of the Red Sea basin and northwestern part of the Arabian Plate. Additional Cenozoic basalt occurs in the Cairo area, west of the western margin of this map (see Bosworth 2015 for details). **b** Compilation of published $^{40}Ar/^{39}Ar$ ages of pre- and syn-rift magmatism in the Red Sea basin (after Bosworth and Stockli 2016) and K-Ar ages in Harrat ash Shaam (after Ilani et al. 2001). Two periods of Oligocene–early Miocene magmatism are distinguishable: (1) initial activity associated with the Afar plume at ~31 Ma, affecting the southern ANS; and (2) syn-rift magmatism along essentially the entire Red Sea rift and northwestern Arabian Plate (Harrat ash Shaam). Widths of boxes indicate published error bars for individual samples except for the Ethiopia and Yemen traps, which are composites of many samples. See Bosworth and Stockli (2016) for sources of data. Lavas in the far north of the Arabian Plate are related to Late Cenozoic collision between the Arabian and Anatolian and Eurasian Plates (Pearce et al. 1990)

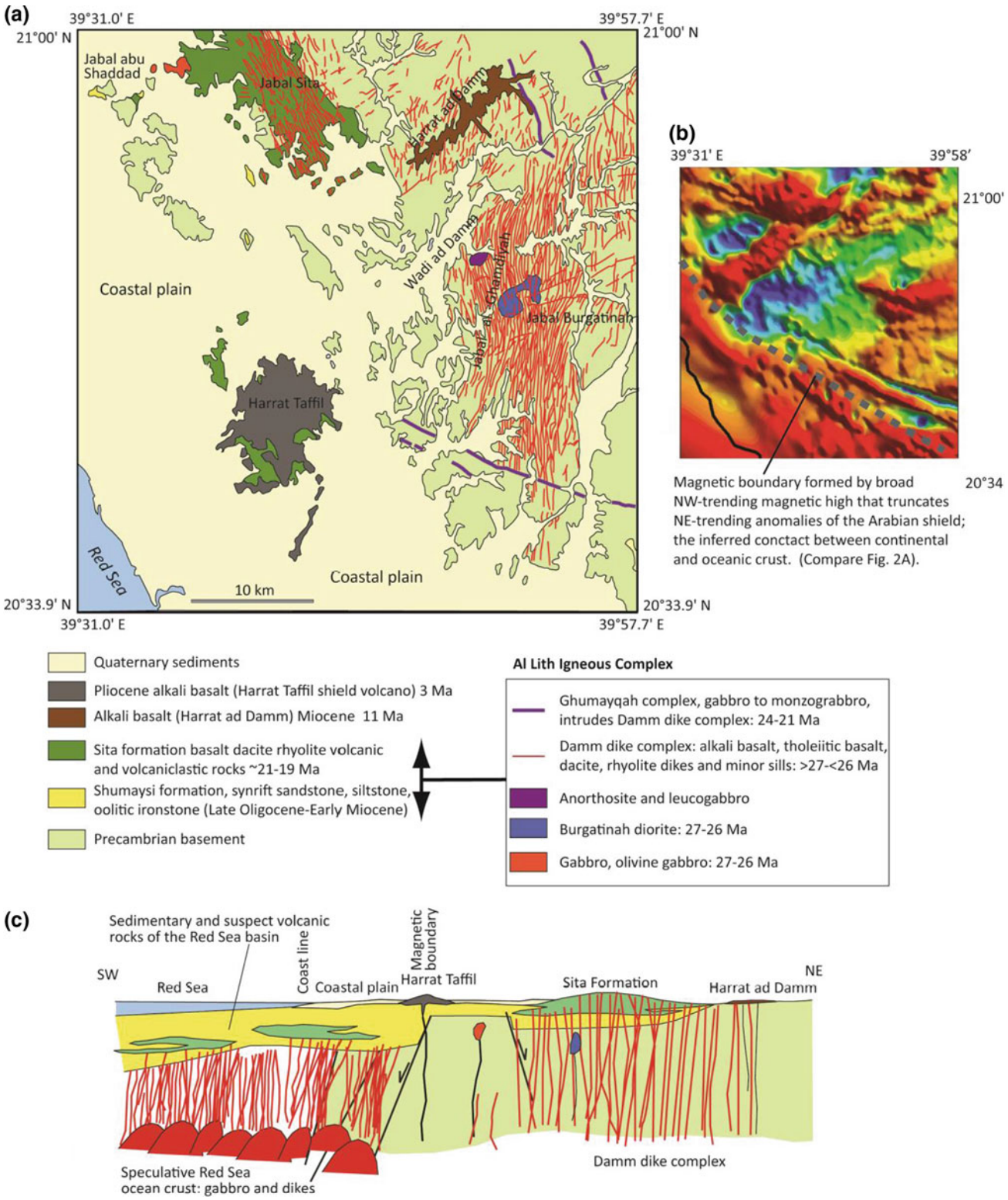

Fig. 6 The Al Lith igneous complex (after Pallister 1987). **a** Map of the complex showing the great concentration of Damm dikes that characterizes the complex. **b** Reduced-to-the-pole aeromagnetic map showing NW-trending linear anomalies coincident with Ghumayqah complex gabbroic dikes and a broad region of high-magnetic intensity in the southwest suggestive of strongly magnetic, possibly oceanic, crust beneath the coastal plain and Red Sea. **c** Schematic paleogeographic reconstruction showing the location of the Al Lith igneous complex in rifted basement of the Arabian Shield at the margin of an inferred swarm of sheeted dikes forming a hypothetical Red Sea crust

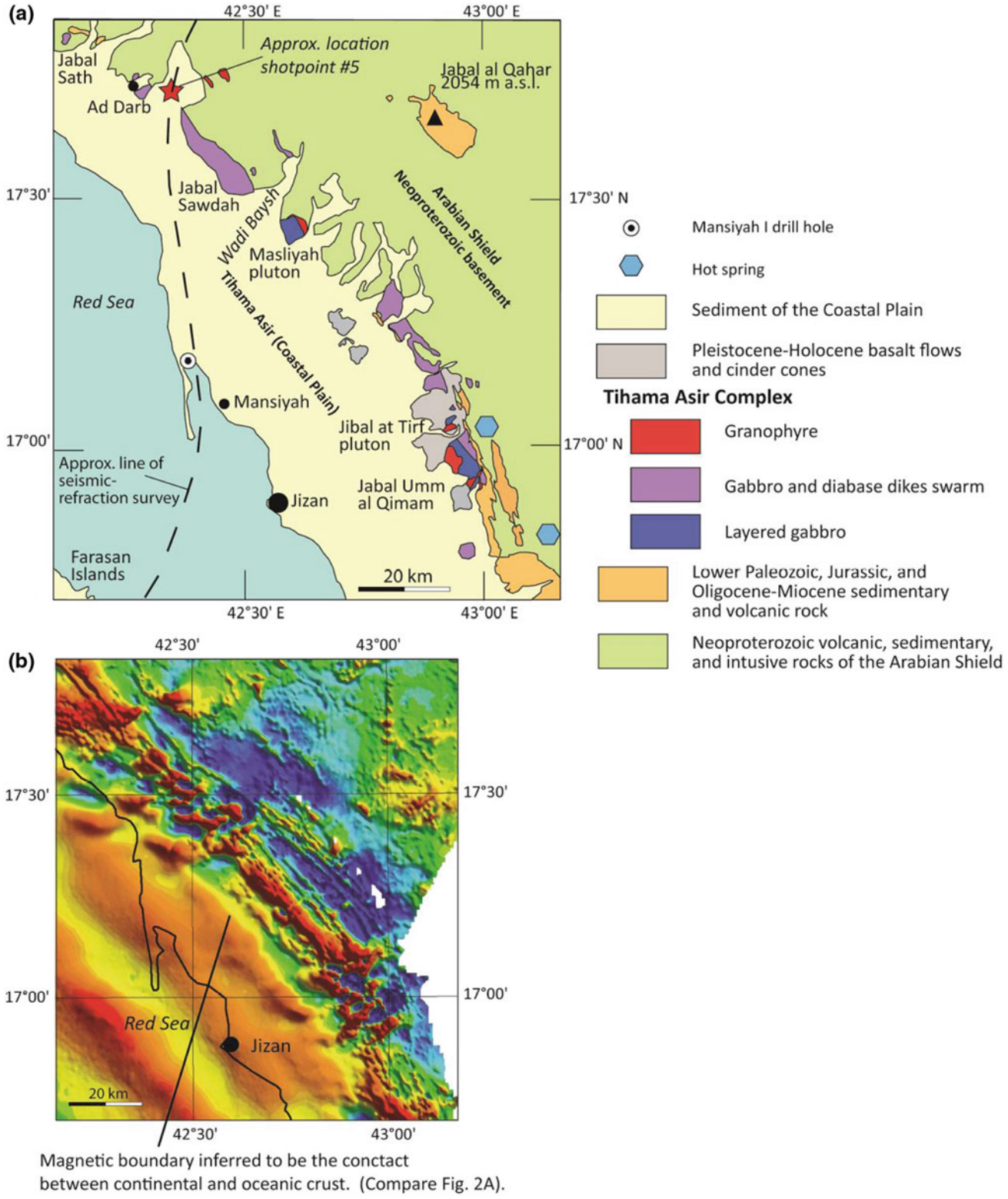

Fig. 7 The Tihama Asir complex (after Coleman et al. 1979 and Blank et al. 1987). **a** Map of the complex showing its strike length of >150 km at the contact between continental crust of the Arabian Shield and Cenozoic sedimentary and volcanic rocks of the Red Sea basin. The complex is partly overlain by Pleistocene-Holocene lava and cinder cones, and details of the contact are obscured by Cenozoic unconsolidated alluvial and eolian sediment. **b** Reduced-to-the-pole aeromagnetic map showing a zone of high-magnetic intensity partly coincident with the Tihama Asir complex and broader zones of high-to-moderate intensity along the coastal plain and Red Sea interpreted here as indicative of oceanic crust

irregular plutons of granophyre exposed inland from Jizan that intruded faulted and extended continental basement at the contact between the Arabian Shield and the Red Sea basin. It has a strike length of >150 km NW–SE parallel to the trend of the Red Sea. Its outcrop width is 5–10 km, but its coincidence with the NW-trending magnetic high shown in Fig. 7b indicates a minimum subsurface or concealed width of at least 20 km. Conspicuous linear, short-wavelength, NW-trending magnetic anomalies farther east suggest the presence of buried Red Sea dikes of the type known elsewhere along the Saudi Arabian margin. The number of dikes and the dike/country-rock volume ratio increase east to west across the shield/coastal plain contact and the western exposures are virtually entirely sheeted dikes, pillow lava, and volcaniclastic rock (Gettings et al. 1986). Individual dikes of the sheeted dike complex are 0.5–19 m wide and vary in density from 100% in areas of dike-on-dike intrusion to 10% or less in areas where screens of country rocks are present. Many dikes intruded along fault planes or joints in the bedrock. Compositionally they are diabase and basalt, with minor gabbro and rhyolite. Layered gabbro, in which variations in plagioclase, clinopyroxene, and olivine contents define subtle, seaward-dipping layers as much as 1 m thick, crops out in plutons as much as 8 km long and 2.5 km wide (Blank et al. 1987). Granophyre occurs as pods and small plutons that intrude the dikes and gabbro. The complex yields K-Ar ages between 24 and 20 Ma for gabbro and granophyre (Coleman et al. 1972), indicating an early Miocene age for the complex, similar to the age estimated for the Al Lith igneous complex. Since the 1950s, the complex was believed to be located at the boundary between the Arabian Shield and Red Sea basin. This conclusion is supported by the coincidence of a region of abrupt thinning of continental crust at the contact between the Arabian Shield and Red Sea basin shown on the seismic-refraction survey profile (Fig. 3) and the NW-trending magnetic boundary shown in Fig. 7b between a region of heterogeneous, shortwave anomalies to the northeast and a region of broad-wavelength anomalies to the southwest.

4 Continental Crust of the Red Sea Margins

The Arabian-Nubian Shield (ANS) extends 3500 km north-south from southern Israel and SW Jordan to Kenya and some 1500 km east-west from central Saudi Arabia to the Nile in Egypt and Sudan, underlying an area of $\sim 2.7 \times 10^6$ km^2 (Fig. 1, inset). This crust formed between ~880 and ~580 Ma as part of the Rodinia-Gondwana supercontinent cycle, during a ~300 m.y. period of Neoproterozoic magmatic and tectonic evolution that yielded a juvenile tract of continental crust, as the ANS was sandwiched between colliding continental blocks of eastern and western Gondwana. Transpressional convergence coupled with tectonic escape and orogenic collapse produced broadly north-trending shear zones and upright tight folds in the southern ANS and northwest-trending strike-slip shear zones of the Najd fault system in the north (Figs. 1 and 4). By early-Cambrian times, the ANS was part of the East Africa–Antarctic Orogen (EAAO; Stern 1994; Fritz et al. 2013), an orogenic belt that stretched southward through the Gondwana supercontinent along the eastern margin of Africa and across Antarctica. Around the Red Sea, ANS rocks crop out in Sinai, Israel, and Jordan in the north; on the Red Sea western flank in the Eastern Desert of Egypt, the Red Sea Hills of Sudan, and the highlands of Eritrea and northern Ethiopia; and on the Red Sea eastern flank in western Saudi Arabia and the highlands of Yemen.

Exposed ANS is composed of subequal proportions of mostly greenschist-facies volcanic and related immature sediments and intrusive plutons (Fig. 8b) that formed during Tonian-Cryogenian and Ediacaran-earliest Cambrian stages. The earlier stage, ~250 m.y. long, corresponds to an episode of accretionary tectonics dominated by formation of volcanic-arc assemblages and accretion of multiple arcs around the Mozambique Ocean to form proto-continental crust. These rocks are dominated by greenschist-facies volcanic and related immature sedimentary rocks and "I-type" granodioritic intrusions that are characterized by similar U-Pb zircon radiometric ages and Nd model ages. In terms of their petrogenesis, they are juvenile additions to the crust from the mantle as indicated by their isotopic compositions (Stern 2002), and are sometimes referred to as the western arc or oceanic terranes of the ANS (Stoeser and Frost 2006). The later, shorter (~50 m.y.) stage was a period of continental collision, escape tectonics, orogenic collapse, and possible lithospheric delamination; rocks formed during this stage include less-metamorphosed volcanic and sedimentary rocks and widespread granitoid plutons and batholiths (Fig. 4).

Stabilization of the end-Ediacaran ANS crust coincided with shield-wide exhumation, uplift, and the development of a regional angular unconformity (Ram Unconformity of Powell et al. 2014). Uplift possibly resulted from lithospheric delamination coupled with regional compression associated with terminal collision between crustal blocks of eastern and western Gondwana (Avigad and Gvirtzman 2009; Abu-Alam et al. 2011). Subsequent regional subsidence allowed deposition of thick sequences of Cambrian and Ordovician sandstone and siltstone, derived mostly from erosion of the Trans-Gondwana "supermountains" in the south (Squire et al. 2006; Meinhold et al. 2013). Cambro-Ordovician rocks originally extended across the entirety or most of the ANS basement, but have been extensively removed by erosion. Lower Paleozoic sandstone locally crops out on the Saudi Arabian coastal plain as

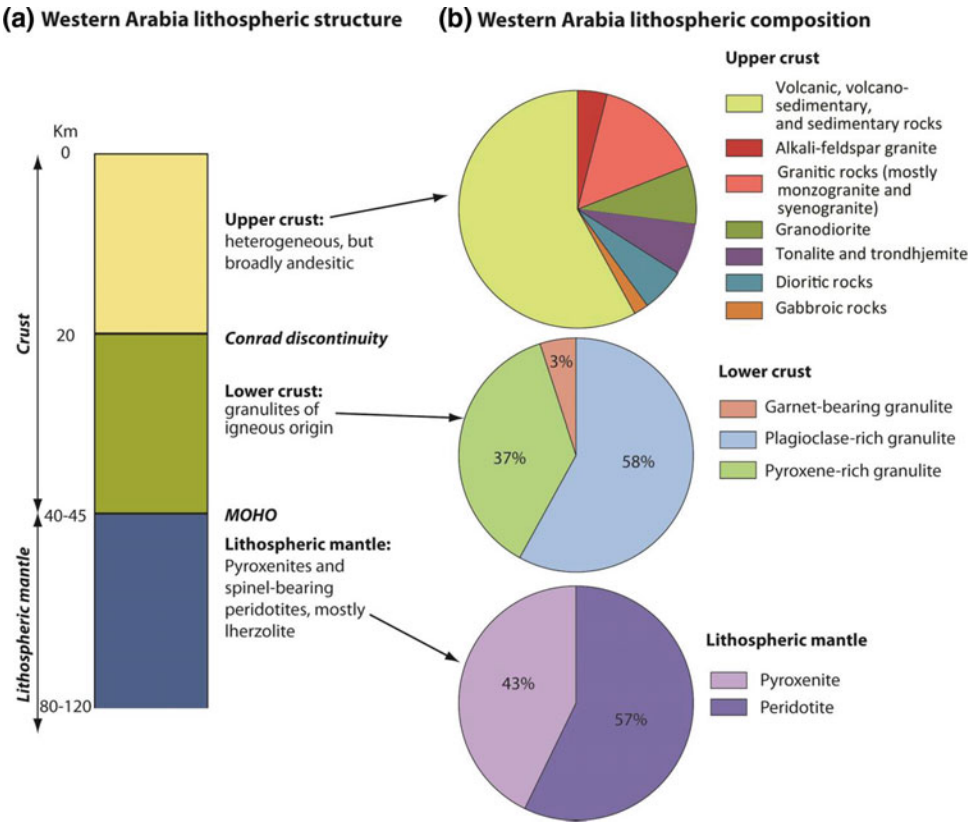

Fig. 8 **a** Structure of western Arabia lithosphere, simplified from Stern and Johnson (2010). **b** Composition of western Arabian lithosphere, as determined from outcrops for upper crust (after Johnson et al. 2011) and reported proportions of lower crust and lithospheric mantle xenoliths brought up in Neogene volcanic eruptions (Harrats; Stern and Johnson 2010). For upper crust, gneiss is calculated in terms of the protolith—thus dioritic gneiss is grouped with diorite, granite gneiss with granite, etc. Ultramafic rocks do not figure either, but amount to about 1%. The Nubian Shield has a similar composition except for a greater proportion of ultramafic rocks

blocks downdropped from their original position at the top of the Red Sea escarpment along seaward-dipping detachment faults (Bohannon 1989), but the main expanse of Phanerozoic rocks east of the Red Sea is 100–700 km inland in central and eastern Arabia. ANS exposures west of the Red Sea extend ~500 km inland in Sudan from the Red Sea coast as far as the Saharan Metacraton (Fig. 1, inset), a region of mainly pre-Neoproterozoic crust that was extensively reworked during the Neoproterozoic (Abdelsalam et al. 2002). To the north, in the Eastern Desert of Egypt, the ANS exposures narrow to less than 100 km.

Tonian-Cryogenian volcanic-arc assemblages constitute tectonostratigraphic terranes that, adjacent to the Red Sea, are referred to as the Eastern Desert, Gebeit, Haya, and Tokar terranes in Egypt, Sudan, and Eritrea, and the Midyan, Hijaz, and Jiddah terranes in Saudi Arabia (Fig. 1). On the basis of isotopic dating and field observations, it is evident that these terranes were once continuous and are now bisected by the Red Sea. The Eastern Desert terrane correlates with the Midyan, the Gebeit terrane with the Hijaz, the Haya terrane with the Jiddah, and the Tokar terrane with the Asir (Fig. 9). The mere fact of correlation, of course, does not itself constrain how close the terranes were juxtaposed prior to Red Sea opening, but the present relationship of the terranes precludes any significant strike-slip displacement of continental crust along the axis of the Red Sea during initiation of Red Sea opening of the type proposed, for example, by Shimron (1989).

4.1 Suture Zones

In addition to the lithostratigraphic terranes that correlate across the Red Sea, there is also general consensus about the correlation of inter-terrane ophiolite-decorated suture zones that resulted from closing the Neoproterozoic ocean basins in which the arc assemblages originated (Azer and Stern 2007; Stern et al. 2004) (Figs. 1 and 9). Of the two ANS sutures that impinge on the Red Sea, the northerly Allaqi-Heiani-Onib-Sol Hamed-Yanbu suture trends E–W to NE–SW across southern Egypt and northern Sudan, and irregularly NE–SW across northwestern Saudi Arabia, forming a composite structure referred to as the YOSHGAH (Yanbu-Onib-Sol Hamed-Gerf-Allaqi-Heiani) suture (Stern et al. 1990). The western part of the suture zone in Egypt and Sudan is a ~400 km-long ophiolite-decorated fold-and-thrust belt composed of imbricate thrust sheets and slices of ophiolite (serpentinite, amphibolite, metagabbro and metabasalt) and island arc metavolcanic/metasedimentary rocks. The Yanbu suture in the Arabian Shield is a similar subvertical to steeply-dipping

shear zone containing nappes and fault-bounded lenses of mafic and ultramafic rocks (Pallister et al. 1988). Radiometric dating of ophiolites, metavolcanic rocks, gabbro, quartz diorite and stitching granites suggests that the ophiolites formed ~730 Ma and that accretion between the Gebeit and Eastern Desert terranes and emplacement of the ophiolitic nappes occurred between 730 Ma and 709 Ma (Ali et al. 2010). The timing of convergence along the Yanbu suture is not precisely constrained, but amalgamation probably occurred at ~700 Ma following 808–721 Ma ophiolite formation, and preceding emplacement of 730–690 Ma granodiorite and tonalite (Pallister et al. 1988). The suture zone in Egypt and Sudan extends to the shield/coastal plain boundary; the Yanbu suture stops some 50 km short of the contact with the Red Sea basin because its continuity is interrupted by granite intrusions.

The Bir'Umq-Nakasib suture, one of the best-exposed Neoproterozoic sutures in the world, is a slightly older zone of amalgamation between the Jiddah-Haya and Hijaz-Gebeit terranes in Saudi Arabia and Sudan (Fig. 9). It extends NE across the ANS as a belt of ophiolite nappes and juvenile metavolcanic, metasedimentary, and intrusive rocks 5–65 km wide and over 600 km long. Dating of ophiolitic rocks, volcanic rocks, and pre- and syntectonic plutons indicates that oceanic magmatism in the region was active ~870–830 Ma and suturing occurred ~780–760 Ma (Abdelsalam and Stern 1993; Hargrove 2006).

The Ad Damm-Barka shear zone is a prominent zone of subvertical shearing and folding at the contact between the Jiddah-Haya and Asir-Tokar terranes. The Barka shear zone is a transpressional duplex made up of at least seven structurally distinct units separated by shears (Drury and de Souza Filho 1988). It dips west between 45° and 80° and is as much as 40 km wide. Each unit has large folds; some are internally imbricated by lesser shear zones. The Ad Damm shear zone is a subvertical fault zone 2–4 km wide extending >350 km NE from the Red Sea coastal plain. It is characterized by dextral strike-slip, moderately to steeply NW-plunging stretching lineations, and conspicuous S–C kinematic indicators in greenschist- to amphibolite-facies phyllite and schist developed from volcanic and volcaniclastic rocks as well as mylonitic gneiss developed from granite of the ~620 Ma Numan Complex. Because shearing deforms the Numan Complex, the age of the youngest finite strain of the Ad Damm fault zone is inferred to be Ediacaran, and the structure is considered by some to be a conjugate shear of the otherwise NW-trending Najd fault system (Hamimi et al. 2014). The Ad Damm-Barka shear zone contains little ophiolite and its tectonic significance is debated; it may be a cryptic suture or a young, dextral strike-slip shear zone superimposed on or obliterating an earlier suture. Importantly, however, both the YOSHGAH and Bi'r Umq-Nakasib sutures and the Ad Damm-Barka shear zone impinge, at various oblique angles, on the Red Sea and create a network of structures and piercing-points that must be put back together in any palinspastic model for the Red Sea (Fig. 9).

4.2 North-Trending Shear Zones

Another distinctive structure in the Asir-Tokar and Jeddah-Haya terranes comprises northerly trending belts of shearing, thrusting, and folding coupled with variable amounts of horizontal strike-slip displacements that resulted from terminal transpressional E–W convergence (Abdelsalam and Stern 1996) (Figs. 1 and 9). These shear zones are marked by chlorite-sericite schist, phyllonite, and local serpentinite schist derived by retrograde metamorphism of the greenschist and amphibolite-facies country rocks. They have a marked lithologic and rheologic contrast with the unaltered country rocks, and constitute north-trending zones of potential crustal weakness. The shear zones are subparallel to the Red Sea dikes, the dike swarms of the Al Lith and Tihama Asir igneous complexes, and to the general trend of the southern Red Sea coastline. Consequently, it is likely that such pre-existing Neoproterozoic structures exercised a geometric control on rifting in the southern Red Sea.

Such shear zones are exposed in the Ghedem area of Eritrea, immediately adjacent to the Red Sea coastline (Ghebreab et al. 2005). The basement rocks here include domes of low- to middle-crustal gneiss and schist metamorphosed to amphibolite facies during progressive syn-deformation metamorphism that peaked at ~590 Ma when *P–T* conditions were near 12 kbar and 650 °C. Structurally, the domes are characterized by low-angle, mylonitic ductile shear zones. Subsequent exhumation of the high-grade rocks and extension along E–ESE- and W–WNW-directed low-angle faults during ANS orogenic collapse are denoted by retrogressive metamorphism between 580 and 565 Ma ($^{40}Ar/^{39}Ar$ hornblende and mica ages) (Fritz et al. 2013). The high-grade rocks were further exhumed during Permo-Carboniferous times and were further thinned from a thickness of ~35 to ~14 km during the Cenozoic by low-angle normal faulting. The Cenozoic faults sole-out into detachments among the low-angle Neoproterozoic mylonites, suggesting that the Cenozoic faults reflecting Red Sea extension exploited, or were controlled by Neoproterozoic structures. Unfortunately, $^{40}Ar/^{39}Ar$ cooling ages of hornblende and muscovite fail to constrain the age of detachment, possibly because this occurred below the closing temperature of muscovite (Ghebreab et al. 2005).

The Gebeit terrane contains the Hamisana and Oko shortening zones (Abdelsalam 1994, 2010; Abdelsalam and Stern 1996) (Ha and On in Fig. 1) that formed between ~660–560 Ma (Miller and Dixon 1992; Stern et al. 1989a,

b). The Hamisana shortening zone extends north across the YOSHGAH suture, which it displaces by about 50 km (Stern et al. 1990), into the southernmost Eastern Desert terrane and impinges the Red Sea coastline at an acute angle. The correlative Hanabiq shear zone, a belt of highly strained rocks >35 km long and nearly 5 km wide, in the Arabian Shield north of Yanbu (Hn in Fig. 1) (Duncan et al. 1990), contains mylonitic gneiss and schist with dextral kinematic markers and syntectonic granitoids that yield a U-Pb zircon age of 590.5 ± 2.8 Ma (Kennedy et al. 2010) interpreted as the time of syntectonic intrusion. Deformation on the Hanabiq shear zone is estimated to be ~610–585 Ma, overlapping the time of movement on the Hamisana shortening zone. The Hanabiq shear zone is evidently a continuation of the Hamisana shortening zone and the two structures constitute another set of piercing-points for modeling Red Sea closure.

4.3 Najd Shear Zones

The northern ANS terranes lack the N–S shortening structures of the southern ANS. Instead, they are pervasively affected by NW-trending "Najd" shear zones (Sultan et al. 1988) that developed in association with northward-directed tectonic escape of the ANS during terminal collision of E and W Gondwana (Burke and Sengor 1985) and created prominent NW-trending brittle-ductile fault zones (Fig. 1). The Najd system, dating between ~620 and 580 Ma, is one of the largest shear zone systems on Earth (Stern 1985) and constitutes a zone of deformation, sometimes referred to as the Najd fault corridor, that extends across the entire Arabian Shield and northern Nubian Shield.

The composition of mid-level ANS crustal rocks includes upper amphibolite-facies quartzofeldspathic (granitic) gneisses and amphibolites exposed in the Meatiq and Hafafit domes in the Central Eastern Desert of Egypt, the Qazzaz dome in northwestern Saudi Arabia and elsewhere (Fig. 4). These rocks crop out in structural highs surrounded by greenschist-facies ensimatic arc rocks and younger sedimentary basins intruded by dioritic, granodioritic, and granitic plutons, and are interpreted as examples of high-grade and migmatitic infrastructure of the mid-crust ("Tier 1" of Bennett and Mosley 1987) that poke through lower grade superstructure rocks ("Tier 2" of Bennett and Mosley 1987). High-strain mylonitic zones separate the high-grade and low-grade rocks and form a system of crustal dislocations referred to, in the Nubian Shield, as the Eastern Desert Shear Zone (EDSZ) (Andresen et al. 2009, 2010) that is related to ~600 Ma Najd faulting. Similar types of crustal vertical heterogeneity are referred to by Blasband et al. (2000) and Fritz et al. (2002), who describe metamorphic belts in Wadi Kid in Sinai and the Sibai and Meatiq regions of the Central Eastern Desert, Egypt as core complexes. The exhumation of the ANS infracrustal rocks in these localities may reflect interaction of Najd left-lateral strike-slip shearing, extension and partially molten middle crust (Stern 2017). Because of their relatively high metamorphic grades and schistose and gneissic fabric, the ANS infracrustal rocks in Egypt were earlier interpreted as remnants of pre-Neoproterozoic continental crust (e.g., Habib et al. 1985; El-Gaby et al. 1988, 1990). However, the absence of significant geochemical, geochronologic, or isotopic differences between the high- and low-grade rocks strongly supports the view that rocks of the two tiers represent different thermal regimes experienced by different levels of Neoproterozoic ANS crust and are further evidence that the ANS crust in its entire thickness is juvenile.

The Najd system is associated with Neoproterozoic pull-apart volcanosedimentary basins located at bends or jogs in the faults and provided a mechanism for the exhumation of mid-level crustal rocks in gneiss domes or core complexes (Fritz et al. 2002; Abd El-Naby et al. 2008; Meyer et al. 2014). Because the Najd structures are so long and form a network of shears that obliquely intersect the Red Sea coastline, they are particularly useful geologic features for constraining palinspastic reconstruction of the ANS before Red Sea opening. Sultan et al. (1988) (using different names to those used here) correlate specific strands of the Najd system across the Red Sea, linking the Qazzaz and Duwi shears and Ajjaj and Nugrus shears for example. Correlations at the level of such detail may be debated, but the general extension of the Najd fault system from the Arabian Shield into the Nubian Shield is without doubt, and must be accommodated in any model of Red Sea closure. Furthermore, Cenozoic rejuvenation of Najd faults controlled the development of the Late Mesozoic-Cenozoic Nakheil and Azlam (Aznam) basins mentioned above. The faults do not appear to cause any jog in the coastline or affect the location of Red Sea deeps, but they do modify Miocene fault geometry and create the Quseir-Duba accommodation zone, a region across which there is a significant change in Red Sea faulting polarity, from NE-dipping Miocene faults to the north to SW-dipping faults to the south (Bosworth 2015).

5 Vertical Structure of ANS Lithosphere

In all discussions of Red Sea opening, it is accepted that the boundary between the Red Sea basin and the ANS crust approximates a major lithospheric discontinuity that marks where once-continuous continental crust was ruptured. Models of continental rifting necessarily entail an understanding of the overall strength of the lithosphere, a rheologic parameter that is generally considered to be controlled

by composition, geothermal gradient or temperature structure (dT/dZ), strain rate, and crustal thickness (Kusznir and Park 1987), along with how much magma was injected (Bialas et al. 2010). Composition affects the rheology of the various layers that make up the lithosphere, and the overall strength of continental lithosphere is considered by some to reflect a relatively strong olivine-rich upper mantle, a weaker granitic to dioritic lower crust, and a stronger upper crust (e.g., Handy and Brun 2004). An alternative view, based on earthquake depth distributions, suggests that the strongest part of the lithosphere is the crust and that the upper mantle is relatively weak (Jackson 2002).

The temperature structure and strain rate of the ANS at the time of rifting is not well established. Limited heat flow data are available from temperatures logged in drill holes at shot points, before explosives were loaded, along the seismic refraction survey conducted in 1974 by the U.S. Geological Survey Saudi Arabian Mission and Saudi Arabian Directorate General of Mineral Resources (USGS/DGMR) from close to Riyadh in the northeast, across the southern Arabian Shield, and finishing at the Farasan Islands in the Red Sea (Fig. 3) (Mooney et al. 1985; Gettings et al. 1986). Together with information from the Mansiyah I deep petroleum exploration drill hole (Fig. 7) (Girdler 1970) and from the Red Sea shelf and axial trough (Girdler and Evans 1977), the data show an apparent increase in heat flow from the Arabian Shield ($\sim$40 mW/m^2) toward the Red Sea margin ($\sim$80–110 mW/m^2). Gettings et al. (1986) account for high heat flow at shot-point 5 close to the Red Sea (Figs. 3 and 7) as the effect of abutting oceanic crust and (or) an enhanced mantle component of heat-flow through the continental crust, which here has been thinned to $\sim$25 km, assuming a temperature regime that has persisted for 10 million years or more.

Comprehensive information about the structure and composition of the ANS lithosphere is given by sources as varied as seismic-refraction surveys, S-wave splitting parameters, lower-crust and upper-mantle xenoliths obtained from Cenozoic lavas (harrats), and structural and lithologic mapping of high-grade rocks exhumed from mid-crustal levels and exposed in gneiss domes or core complexes. One widely accepted model of P-wave arrival times measured during the 1974 Riyadh-Farasan seismic-refraction survey identifies $\sim$40 km thick continental crust divided into an upper $\sim$20 km thick layer of low Vp (<6.5 km/s) of likely felsic composition and a lower $\sim$20 km thick layer of higher Vp (6.7–7.8 km/s) of likely mafic composition (Fig. 3) (Mooney et al. 1985; Gettings et al. 1986). The ANS upper mantle is characterized by high Vp velocities (>8 km/s), suggesting a bulk ultramafic composition. S- and Raleigh-wave functions indicate that the ANS upper (lithospheric) mantle varies in thickness from >40 km at the Saudi Arabian coastline to $\sim$90 km beneath the shield to >170 km just east of the shield (Hansen et al. 2007; Park et al. 2008). Prodehl (1985) modeled the Saudi Arabian crust–mantle boundary at a common depth of 40 km with a maximum of 50 km beneath the southwestern part of the shield and an abrupt thinning to 15 km beneath the Red Sea; a similar result was obtained more recently by Tang et al. (2016). In the Prodehl model, relatively high-velocity material at about 10 km depth in the western shield upper crust is underlain by velocity inversions, and the lower crust with a velocity of about 7 km/s is underlain by a transitional crust-mantle boundary. The upper mantle appears to have a laterally discontinuous lamellar structure with intermixed high-velocity and lower velocity zones.

A limitation of seismic-refraction surveys, of course, is that the results emphasize horizontal structure at the expense of vertical or steep structure. As a consequence, although the Riyadh-Farasan survey clearly shows vertical heterogeneity (layering) in the ANS crust, it provides few instances of conspicuous Vp discontinuities that reflect the many steeply-dipping shear zones and lithologic contacts known to exist in the Arabian Shield (Gettings et al. 1986). The vertical discontinuities that are identified (Mooney et al. 1985) denote a fault in the upper crust $\sim$200 km from the northeastern end of the profile, structures in the upper part of the upper crust southwest of the known Al Amar fault zones, a diapiric structure coincident with the Khamis Mushayt gneiss, and an abrupt thinning of the crust from $\sim$40 km beneath the western edge of the ANS to $\sim$5 km beneath the Red Sea coastal plain (Fig. 3) (Blank et al. 1986; Gettings et al. 1986).

Mafic xenoliths brought to the surface in Cenozoic basalt have been obtained from eight locations in the western part of the Arabian Plate, extending from Harrat Kishb to Harrat ash Shaam (Fig. 5) (see review in Stern and Johnson 2010; Stern et al. 2016). Compositionally, the xenoliths are divided into samples of ANS lower crust and upper mantle on the basis of whether or not the samples contain plagioclase or olivine; plagioclase indicating a lower crustal origin, whereas abundant olivine suggests an upper-mantle origin. Lower crustal xenoliths include mafic granulites, 2-pyroxene gabbro, and rare garnet-bearing granulites. Ten lower crustal xenolith samples from Saudi Arabia yield a mean Nd model age of 0.76 $\pm$ 0.08 Ga (Claesson et al. 1984) indicating that the southern Arabian crustal lithosphere originated during the Neoproterozoic, whereas $\sim$360 Ma and $\sim$560 Ma U-Pb zircon ages of lower crustal samples from Syria and Jordan, respectively, imply that the crust in the northern part of the Arabian Plate is younger (Cadomian and Carboniferous) (Stern et al. 2014, 2016; Golan et al. 2017). Xenolith samples of the upper mantle include spinel lherzolite, dunite, wehrlite, clinopyroxenite, and megacrysts of clinopyroxene and amphibole, representing a suite of peridotite and pyroxenite consistent with the >8 km/s P-wave velocity revealed by the seismic-refraction data.

Another glimpse of mantle structure beneath the Arabian Shield is given by analysis of teleseismic receiver functions and shear-wave splitting (Levin and Park 2000; Hansen et al. 2006) which reveal an upper mantle fabric with anisotropic symmetry axes oriented ~N–S. Levin and Park (2000) suggest that the anisotropy represents shear zones developed during Neoproterozoic continent–continent collision. Hansen et al. (2006, 2007) alternatively argued that neither fossil lithospheric anisotropy nor present-day asthenospheric flow fully explains the observed splitting. They interpreted the splitting as a result of Cenozoic northeast-oriented flow associated with absolute Arabian Plate motion combined with northwest-oriented flow associated with a channelized Afar plume.

6 Discussion

The Red Sea basin is the world's best example of a nascent ocean, juxtaposing well-defined continental and oceanic crusts. It is located between Neoproterozoic crustal blocks of the northeastern Nubian and western Arabian Plates and is the result of rupturing and separation of continental lithospheres.

As described above, the accepted Red Sea model envisages active rifting and emplacement of oceanic crust in the axial region of the southern Red Sea and a transition to a northern region underlain by extended continental crust. In our opinion, however, the geologic, geophysical, and geographic features of the Red Sea strongly support an alternative model in which most of the Red Sea, in the north as well as the south, is underlain by oceanic crust. These features are: (1) the pattern of basement structures that require a virtual coast-to-coast closure of the Red Sea; (2) interpretations of potential field data—gravity and magnetics, that that we find to be compelling in the axial region south of ~22° N, persuasive for the margins of the southern Red Sea, and suggestive of extensive oceanic crust in the northern Red Sea; and (3) the presence of dikes, gabbros, and basalt flows emplaced during the early stages of Red Sea development, which suggest major upwelling of the asthenosphere, partial melting, and intrusion that would have thermally and mechanically weakened the lithosphere and facilitated rupture of the ~40-km thick continental crust and thicker mantle lithosphere that existed prior to Red Sea opening.

Ever since Wegener (1920) there has been a strong opinion that the two plates prior to Red Sea opening were closely juxtaposed, a model referred to by Gettings et al. (1986) as "this venerable concept" and by Coleman (1993), in the context of the reconstruction by Vail (1985), as "the most successful". Wegener (1920) made the proposal because of the close fit of the opposing shorelines, the prominent eastward bend of both shorelines north of Jiddah and Port Sudan, and a westward bend south of Jiddah and Port Sudan (Fig. 1). Palinspastic reconstructions of Precambrian structures across the Red Sea by Abd El-Gawad (1970), Greenwood and Anderson (1977), Vail (1985), and Sultan et al. (1988, 1993) all adopt a close-fit. A variant palinspastic model resulted from a study by the Saudi Geological Survey (SGS) and the Egyptian Mineral Resource Authority (EMRA) designed to test the hypothesis of a virtual coast-to-coast closure in the northern part of the Red Sea (Kozdroj et al. 2011). Although existing geologic maps, rock descriptions, and geochronological results suggested that rock units and structures (piercing-points) on one side of the Red Sea had counterparts on the other side, the investigation revealed that no unique one-to-one correlation of rock units could be made and structural misfits remained. It was concluded that a reconstruction based on tightly fitting the present shorelines was not satisfactory and at least a 15–30 km gap should be left between them, representing an area covered by Cenozoic sediments and underlain by unknown Neoproterozoic rocks (Kozdroj et al. 2011).

The conclusion of Kozdroj et al. (2011) runs counter to the view of the northern Red Sea as being underlain by stretched continental crust, but it is the best way to fit correlative ANS basement rocks and structures on either side of the Red Sea. This fit is the primary reason we also argue for a relatively tight pre-Red Sea juxtaposition of the Arabian and Nubian Plates (Fig. 9). As noted above, the correlative basement structures intersect the Red Sea coastlines at orientations ranging from approximately orthogonal to acute. Structures oblique to the Red Sea provide particularly tight reconstruction constraints because bringing such structures into alignment is very sensitive to minor differences in back rotation. Structures that intersect the Red Sea at high angles are much less sensitive to such small differences in rotation and so are correspondingly less useful in constraining how the Red Sea should be palinspastically closed. Nevertheless, the integrated network of basement structures strongly supports a tight fit of the Arabian and Nubian Plates. Sultan et al. (1993) proposed a similar fit on the basis of juxtaposing satellite imagery (Fig. 10) and our Fig. 9 uses the same pole of rotation to juxtapose the Arabian and Nubian Plates. As in the proposal by Sultan et al. (1988), we envisage that the Qazzaz shear zone has a counterpart in shear zones in the Duwi area; the Ajjaj shear zone continues in the Nugrus shear; the Hamisana shortening zone meets the Hanabiq shear zone; the Sol Hamed sector of the YOSHGAH suture matches up with the Yanbu sector; the Bi'r Umq suture joins with the Nakasib suture, the Ad Damm fault continues in the Barka shear zone, and shear zones in the Asir terrane align with shear zones in the Tokar terrane.

Although Kozdroj et al. (2011) were not able to make one-to-one correlations between ANS rock units on the margins of the northern Red Sea, we note a close

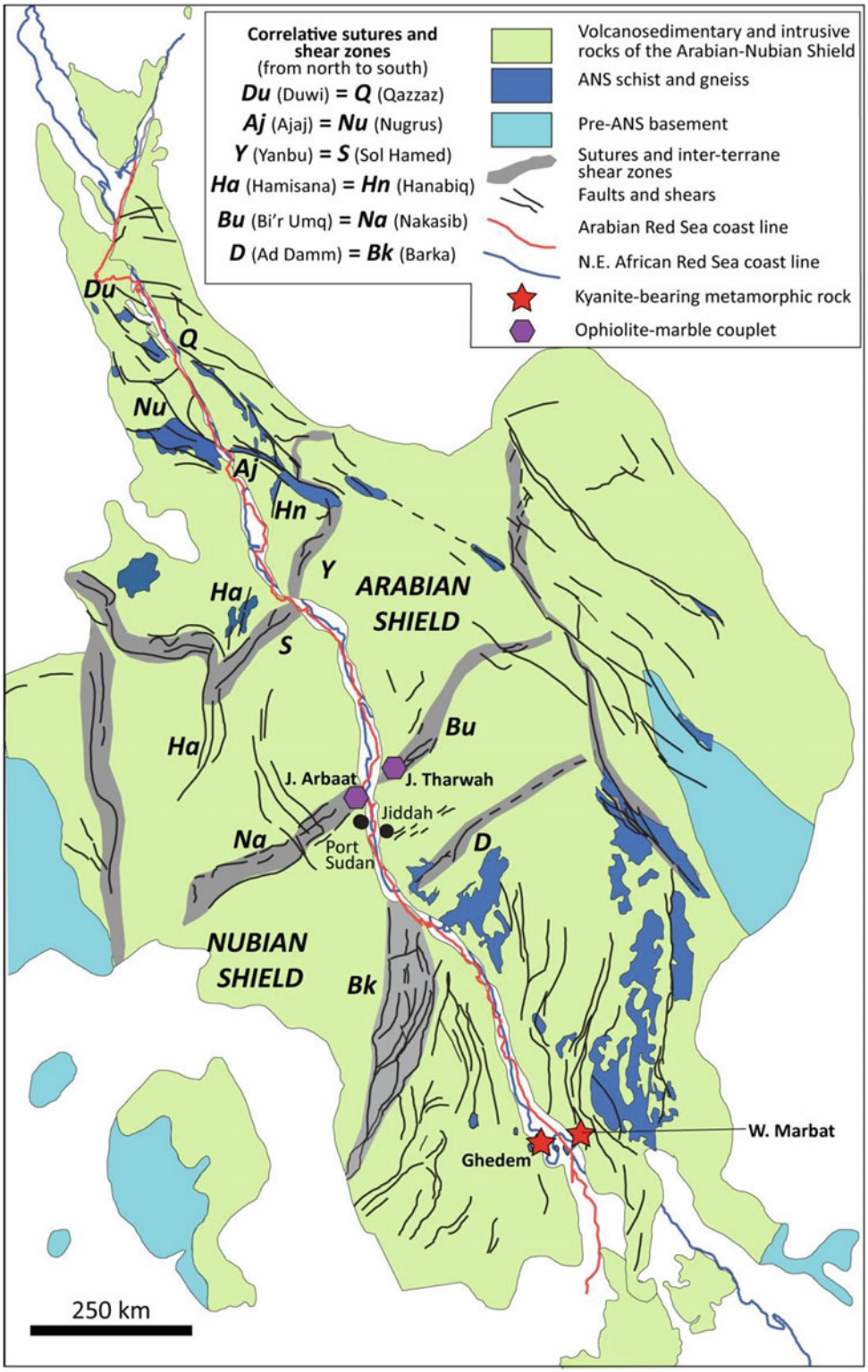

Fig. 9 Preferred palinspastic reconfiguration of the pre-Red Sea rifting relationship of the Arabian and Nubian Shields, showing a near coastline to coastline closure based on the alignment of major structures (sutures and shear zones) in the basement. The configuration is the same as that shown in Fig. 10

juxtaposition of distinctive lithologies in at least two regions on either side of the southern Red Sea, compatible with the reconstruction proposed here. One set of lithologies consists of ophiolite and marble that crop out as components of the Bi'r Umq-Nakasib suture on either side of the Red Sea. The ophiolites are exposed as nappes in Jabal Tharwah in the east and Jabal Arbaat in the west (Fig. 9), underlain in their respective footwalls by thick units of marble. The resulting lithologic couplet—ophiolite and marble—crops out in mountains immediately adjacent to the coastal plain on

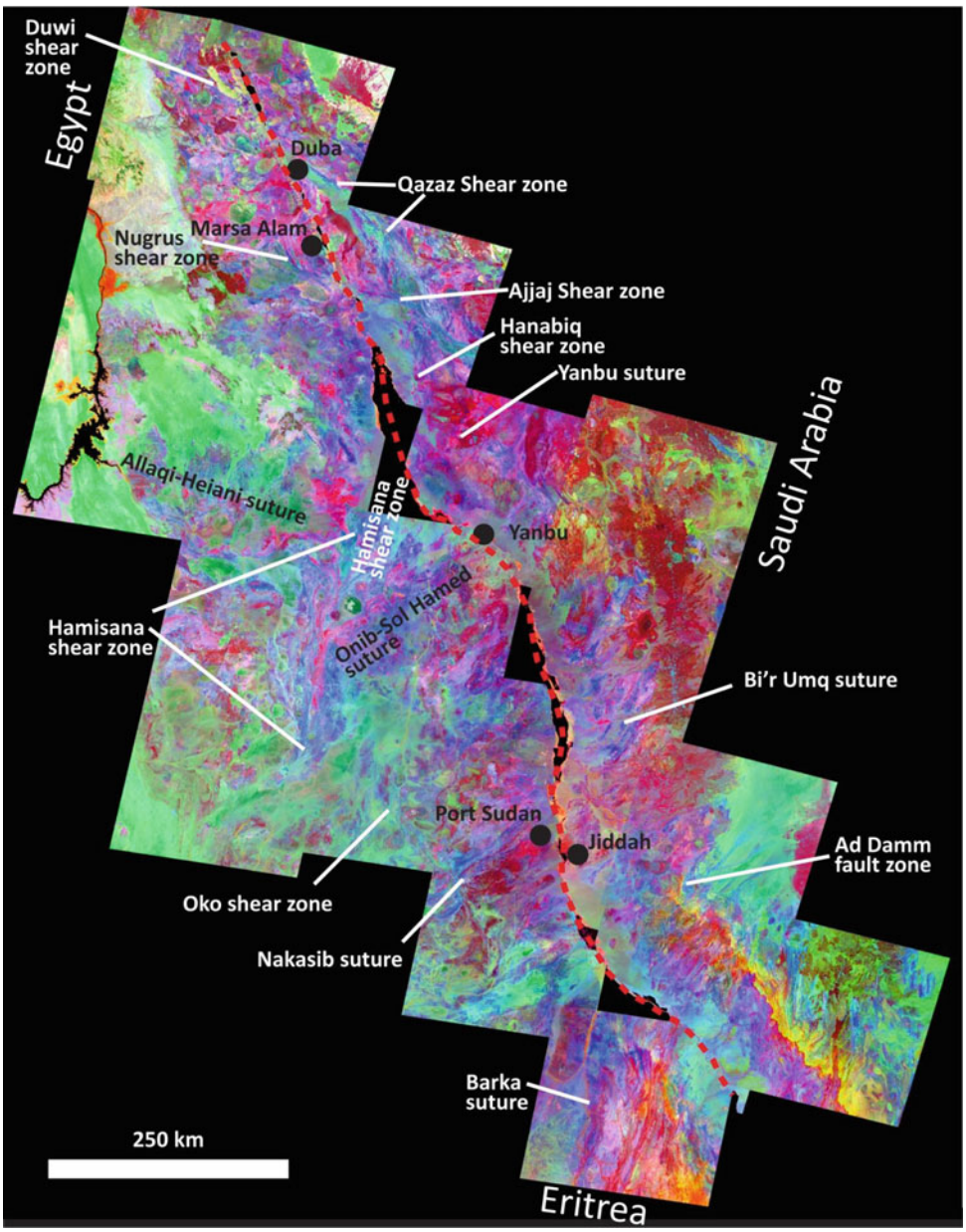

Fig. 10 Colour composite of 23 Landsat thematic mapper scenes (each 185 × 185 km), from Sultan et al. (1993). Dashed red line is preferred closure of Red Sea, near coastline-to-coastline, required to bring structures of the Arabian and Nubian Shields into alignment. The Arabian and Nubian shields were restored to our preferred pre-Red Sea configuration by rotating the Arabian plate around by 6.7° around a pole positioned at 34.6° N, 18.1°E (Note that this is very close to present rotation pole at 32.8°N, 23.8°E (DeMets et al. 2010)). Note that 6.7° of rotation at present rate of 0.38°/Ma would take 17.6 Ma. Restoration is based on matching ANS structures on either side of the Red Sea. TM band ratio product 5/4 × 3/4 (sensitive to the abundance of Fe-bearing aluminosilicates) is assigned blue, band 5/1 (sensitive to the abundance of opaque minerals such as magnetite) is assigned green, and band 5/7 (sensitive to the abundance of hydroxyl- and carbonate-bearing minerals) is assigned red

either side of the Red Sea. A palinspastic reconstruction of the type proposed here would place the lithologic couplets in virtual contact. Farther south, another set of distinctive rock units would be brought within a few tens of kilometres juxtaposition by our preferred reconstruction. The rocks—kyanite-bearing metasediments—crop out in the Ghedem area, Eritrea, and in Wadi Marbat on the Red Sea margin 80 km north of Jizan, Saudi Arabia. In the Ghedem area, the kyanite-bearing rock is paraschist, composed of kyanite, staurolite, almandine garnet, biotite, and quartz derived from a pelitic protolith (Beyth et al. 1977). At Wadi Marbat, the kyanite-bearing rock is kyanite-topaz-lazulite gneiss associated with andalusite-bearing hornfels and quartz-sericite schist that may have originated by high-pressure hydrothermal alteration of pelitic sedimentary rock (Collenette and Grainger 1994). Kyanite-bearing rocks are uncommon in the ANS, being confined to some ten locations in the Arabian Shield (Collenette and Grainger 1994) and in the Nubian Shield to metamorphic core complexes in Egypt and kyanite gneiss in the Duweishat area of northern Sudan. Exposures of kyanite in basement rocks close to both western and eastern contacts of the ANS with the Red Sea basin are therefore noteworthy as a possible piercing-point across the Red Sea.

The satellite imagery shown in Fig. 10 (after Sultan et al. 1993) illustrates the continuity of ANS structures achieved by closing the Red Sea in our preferred ANS reconstruction. In this figure, the Arabian and Nubian Shields were restored

to a pre-Red Sea configuration by rotating the Arabian Plate 6.7° clockwise around a pole positioned at 34.6°N, 18.1°E (Sultan et al. 1993). Such a rotation at the present rate for the Arabian Plate of 0.38°/Ma would take 17.6 Ma. This pole is very close to the rotation pole at 32.8°N, 23.8°E more recently determined by DeMets et al. (2010) on the basis of a global assessment of best-fitting angular velocities for the geologically current motions of 25 tectonic plates.

Furthermore, the ANS structures not only help constrain models of Red Sea closure, they also provide insight into Red Sea geometry. As commented earlier, the Red Sea was initiated by propagation of plume-related magmatism northward from the Afar region. Such magmatic extension would have penetrated continental lithosphere, in the region north of Afar, dominated by a N–S structural grain in which zones of shearing and retrogressive metamorphism constituted zones of weakness. We propose that the structural grain of the ANS, at least south of 20°N, was a major factor in controlling the trend of the southern Red Sea by localizing Red Sea extensional faults. It is interesting to note, furthermore, that the upper-mantle anisotropy symmetry axis recognized by Levin and Park (2000) also trends N–S and is explained by Levin and Park as the effect of shear zones developed in the ANS during terminal Neoproterozoic continent–continent collision. This raises the intriguing possibility that there is a causal link between the structure of the upper mantle and trend of the southern Red Sea, as well as between the crust and the Red Sea.

To the north, in the region between latitudes ~20°N and 24°N, the Red Sea axis and coastlines are characterized by sigmoidal bends. This part of the Red Sea is north of the region dominated by north-trending shear zones, but instead is bracketed by the YOSHGAH and Bi'r Umq-Nakasib sutures. As noted earlier, these structures are somewhat orthogonal to the Red Sea trend and therefore would not have directly controlled it. However, they would have constituted zones of lithospheric weakness and they may have indirectly controlled rifting geometry in the manner of tectonic inheritance at a passive margin of the type described, on a larger sale, to account for bends in the eastern North American continental margin during the opening of the Iapetus and Atlantic Oceans (Thomas 2006). The NW-trending Najd structures that dominate the ANS continental crust north of 24°N had little effect on the trend of the notably linear Red Sea and its coastlines. This may be due to the flattening of Najd shears above hot Tier 1 upper crust (Stern 2017), so that they did not penetrate deeply enough into the lithosphere to form significant zones of weakness; alternatively, the Najd shears were annealed by Ediacaran igneous intrusions long before Red Sea opening. The Najd faults, however, helped to localize Cenozoic sedimentary basins that indent the basement exposures in Egypt and Saudi Arabia, and create the Quseir-Duba accommodation zone of faulting in the Red Sea (Bosworth 2015).

The degree of closure accepted for the Red Sea is important because it has a direct bearing on interpretations about the composition of the Red Sea crust, namely that different closures are expected if the Red Sea is underlain by stretched continental crust or Cenozoic oceanic crust. A simple estimate that the Red Sea is underlain by continental crust stretched to $\beta = 2$ implies that basement structures on unrifted crust in NE Africa and Arabia would realign when the Red Sea, presently ~300 km wide, is closed to ~150 km width. In contrast, a Red Sea crust composed of newly emplaced Cenozoic igneous rocks would permit a virtual coastline-to-coastline closure and a tight fit of basement structures.

The alignments of basement structures presented here strongly favour a near coast-to-coast closure of the Red Sea and a model that most if not all of the Red Sea is underlain by oceanic crust. This situation is widely accepted for the southern Red Sea. Short wavelength Vine-Matthews magnetic anomalies along the axial trough south of 22°N provide unequivocal evidence for the emplacement of oceanic crust under the central part of the southern Red Sea, and the presence of broader wavelength, but similarly NW-trending anomalies to the east is permissive of oceanic crust beneath the Red Sea margins as well. Farther inland, the Al Lith and Tihama igneous complexes testify to the emplacement of new igneous material on the margins of the Red Sea, and are consistent with a transition from continental to oceanic crust close to the shoreline in a region where seismic-refraction profiling indicates that the crust changes abruptly in thickness from ~40 km inland to 5 km beneath the Red Sea shelf (Mooney et al. 1985) (Fig. 3) and where regional magnetic boundaries testify to abrupt changes in crustal lithology.

The nature of the northern Red Sea crust is more contentious. As considered by Bosworth (2015), the similarity of Miocene stratigraphy in the northern Red Sea and Gulf of Suez, established by petroleum exploration drilling, is a strong argument in favor of extrapolating models for development of the Gulf of Suez to the northern Red Sea. However, the geophysical interpretations of Hall et al. (1977) and Saleh et al. (2006), for example, strongly favor a conclusion that the northern Red Sea crust contains much more oceanic material than is considered in the conventional interpretation.

If the Red Sea is modeled as largely underlain by oceanic crust in the south and to an unknown but significant degree in the north, an immediate question concerns how the ANS continental crust ruptured and separated to accommodate oceanic crust? As quantitatively modeled by McKenzie (1978), lithospheric extension and rift evolution reflects two

phases, extension and subsidence. Rapid stretching thins the lithosphere and allows passive upwelling of hot asthenosphere. This stage is associated with normal faulting and tectonic subsidence. Once extension stops or localizes at a new mid-ocean spreading ridge, the stretched lithosphere cools and re-thickens, accompanied by slow "thermal" subsidence. This model has been applied to rifts all over the world. It is applied to the East African Rift and the Gulf of Suez (e.g., Bosworth 2015; Fig. 11a) and is implicit in models calling for the northern Red Sea to be largely underlain by stretched continental crust (Fig. 11b).

However, one problem arising from applying a stretching model to the Red Sea is the considerable strength of ANS lithosphere. Regardless of the relative importance of a strong or weak upper mantle in controlling lithospheric rheology, the Neoproterozoic-Cadomian age and mafic nature of ANS lower crust would make it cool, strong, and difficult to stretch. A solution to this problem comes from understanding the importance of dike injection as a mechanism that weakens and ultimately allows rupture of otherwise strong lithosphere (Bialas et al. 2010). This has been assessed recently by Ligi et al. (2015) to account for rupture of continental crust and initiation of seafloor spreading in the central part of the Red Sea. Ligi et al. (2015) envisage that the initial phase of continental lithospheric thinning by normal faulting was accompanied by asthenospheric upwelling which resulted in melting at the mantle-crust boundary and underplating of the crust by gabbro. Subsequent weakening of the lithospheric mantle and concomitant injection of gabbroic and basaltic dikes ruptured the lithosphere; mantle partial melting generated mafic magmas that were extracted at the rift axis forming shallow gabbro intrusions, dikes, and basaltic lava. Ligi et al. (2015) see evidence for their model in the swarms of dikes that run the entire length of the eastern Red Sea coast and in the high-pressure gabbro exposed on Zabargad Island and low-pressure gabbroic intrusions and basaltic dikes found on the Brothers Islands off the coast of Egypt. Following modeling by Saleh et al. (2006), we propose that gabbros and dikes representing oceanic crust underlie much or most of the shelf regions of the Red Sea as well as its axial region. Given these thermal and intrusive processes, it is likely that, at its initiation, rifting in the thick, cool, and strong NE-African-Arabian lithosphere resulted in a narrow zone of localized strain of the type described by Kearey et al. (2009), but subsequent thermal weakening of the lithosphere would lead to widening of the zone of strain. The asymmetry of the Red Sea basin shown by more basaltic flows and dikes and greater rift flank elevations in Arabia than NE Africa has been seen as evidence for rifting in terms of simple shear extension on an east dipping, low-angle master fault that penetrates the lithosphere (Dixon et al. 1989) although the model of Ligi et al. (2015), for example, envisages symmetrical extension at the continental to oceanic transition.

On the basis of our interpretation that the Red Sea is largely underlain by oceanic material, is part of a magmatic province, and that dike intrusion was important for weakening and rupturing the lithosphere, we tentatively propose that the Red Sea is a volcanic rifted margin (VRM). The VRM concept derives from modern interpretations of continental breakup that emphasize great magmatic outpourings at the time of rifting. The VRM concept was, in fact, being developed in the early 1980s at about the same time that Red Sea models emphasizing continental stretching were articulated, but for unknown reasons did not get applied to the Red Sea. The VRM concept was triggered by

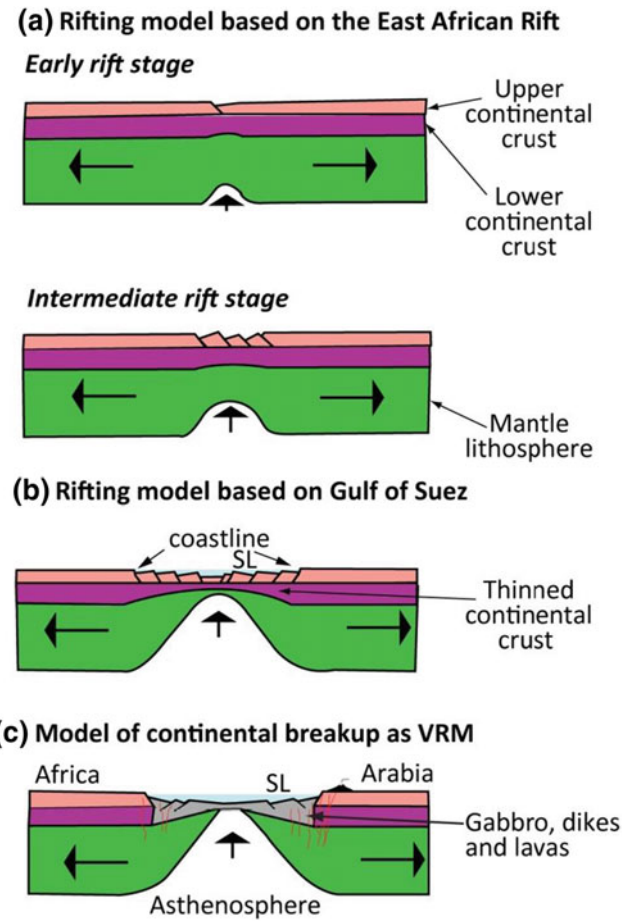

Fig. 11 Models of continental rifting. **a** Continental rifting and breakup based on our understanding of the East African Rift and Gulf of Suez. Early Rift Stage as in the East African Rift; in the initial stage of rifting, continental crust and underlying mantle lithosphere stretches. Intermediate Rift Stage; in this stage continued crustal thinning by normal faulting and lithosphere extended, as experienced by the Gulf of Suez during the Oligocene. **b** Model of a mature rift stage based on the conventionally understood geology of the Gulf of Suez and northern Red Sea, showing thinned continental crust and mantle lithosphere beneath marine basin. **c** Continental breakup with a marine basin underlain by a volcanic rifted margin; our proposed model for the northern Red Sea

recognition of seaward-dipping layered seismic reflectors in the upper oceanic crust offshore Norway, which Mutter et al. (1982) interpreted as a layered igneous sequence formed at the earliest stage of North Atlantic opening. It is interesting to note that Norwegian coastal regions contain little or no evidence that a VRM exists offshore even if rift-flank crust is exposed; for example, the onshore part of the ~55 Ma Norwegian VRM has no exposed lavas, dikes, or plutons despite the nearby presence of a massive offshore igneous construction. Prior to the work by Mutter et al. (1982), crust marking the transition from continent to ocean—which forms at the time of continental breakup and is buried beneath thick sedimentary sequences of passive continental margins—was thought to be overwhelmingly composed of stretched continental crust. At the present time, the VRM paradigm is the dominant model for continental breakup and ~90% of all passive continental margins are now thought to be VRMs to varying degrees (Menzies et al. 2002).

A model for the crust beneath Red Sea evaporites as a VRM is depicted in Fig. 11c, in contrast to models of Red Sea continental rifting and breakup based on our understanding of the East African Rift and Gulf of Suez. It is interesting to note that thirty years ago, McGuire and Coleman (1986) explicitly compared the Tihama Asir complex to the tholeiitic gabbro and syenite intrusions and dike swarms of East Greenland, which are now accepted as a prime example of a VRM (Voss and Jokat 2007). Emplacement of dikes as well as kilometre-scale thicknesses of basaltic and rhyolitic volcanic formations figure in the VRM model proposed for the onset of rifting in the Afar (Wolfenden et al. 2005). We acknowledge that the volume of magmatic material exposed on the margins of the Red Sea is considerably less that that present in Afar, but if dike intrusion was important for weakening and rupturing the lithosphere, then a VRM interpretation for the Red Sea becomes an attractive interpretation as an alternative to the conventional continent-ocean transition model.

Exceptions to the VRM model occur. The Portugal continental margin is known to lack a VRM (Manatschal 2004). A key factor in support of the Red Sea as a VRM is its obvious association with magmatism. Oceanic magmatism created accreted oceanic crust in the southern part of the present-day axial trough and, depending on interpretation of magnetic striping and the tectonic significance of dike-on-dike intrusions, across the entire southern sea and parts of the coastal plain. Elsewhere on the Red Sea ANS margin continental magmatism created extensive lava fields (harrats). Continental volcanism began in Ethiopia and Yemen ~31 Ma and continued between 24 and 23 Ma along the eastern margin of the Red Sea and in the subsurface near Cairo. A major episode of mafic diking affected Sinai and NW Arabia at 20–24 Ma; a slightly larger range (21–28 Ma) is found for intrusive rocks and dike swarms near 21°N in coastal Arabia.

If a VRM model applies to the Red Sea crust, it probably formed ~20–24 Ma ago, when the basin-wide basaltic volcanism occurred. Early Miocene igneous activity was characterized by tholeiitic basalts, indicating high-degree (10–20%) mantle melts comparable to those that characterize other VRMs. Early Miocene magmas differed in this regard from low-degree (1–5%) mantle melts of basanite and alkali basalt, which erupted more recently in the basalt fields (harrats) to the east. The 20–24 Ma (K-Ar age) sequence of layered gabbro, granophyre, and dike swarms at Tihama Asir in the southern Red Sea coastal region and similar igneous rocks at Al Lith could well be exposed Red Sea VRM. Offshore seismic profiling designed to image beneath the salt followed by drilling to basement in the Red Sea is required to test these ideas.

7 Conclusion

The correlation of Neoproterozoic structures and lithologies across the Red Sea strongly favors a model in which the Red Sea crust is predominantly Cenozoic oceanic material and in which NE Africa and the Arabian Peninsula were originally closely juxtaposed. A model of this type suggests the Red Sea contains minimally stretched continental crust and identifies the Red Sea as a Volcanic Rifted Margins (VRM). It is now recognized that continental breakup often involves great magmatic outpourings and almost 90% of all passive continental margins are now thought to be VRMs (Menzies et al. 2002). By considering the known ages of tholeiitic igneous activity on the margins of the Red Sea basin, we suggest that the Red Sea VRM formed ~20–24 Ma ago. Early Miocene tholeiites around the Red Sea indicate high-degree (10–20%) mantle melts like those of other VRMs. The 20–24 Ma sequence of layered gabbro, granophyre, and dyke swarms at Tihama Asir in the southern Red Sea coastal region (McGuire and Coleman 1986) is likely exposed Red Sea VRM. The emplacement of gabbro and dikes associated with the formation of oceanic crust provides a mechanism for rupturing strong ANS lithosphere by magmatic weakening of the lithosphere and accounts for the magnetic stripes along the Red Sea axial trough as well as under the Red Sea marginal sedimentary basins and coastline. It appears that the northerly trend of the southern Red Sea was controlled by the N–S trending structural fabric of the basement. We concur with previous authors that the bend in the Red Sea between 20°N and 24°N is a consequence of preexisting zones of crustal weakness orthogonal to the Red Sea represented by the YOSHGAH and Bi'r Umq-Nakasib sutures and the Ad Damm-Barka shear zone.

We likewise concur with inferences by other authors that the Najd fault system in the north strongly affected Cenozoic Red Sea faulting.

Acknowledgements We are grateful to Dr. Zohair Nawab and Dr. Najeeb Rasul of the Saudi Geological Survey for organizing the second workshop on the Red Sea in Jeddah in 2016 that gave us the occasion to consolidate our ideas about the initiation of the Red Sea and thank Springer-Verlag for publishing this paper as part of the workshop proceedings. We greatly appreciate the critical comments and suggestions of three anonymous referees. This is UTD Geosciences contribution # 1299.

References

Abd El-Gawad M (1970) Interpretation of satellite photographs of the Red Sea and Gulf of Aden (with discussion). In: A discussion of the structure and evolution of the Red Sea and the nature of the Red Sea, Gulf of Aden and Ethiopia rift junction. Phil Trans R S London Ser A 267:23–40

Abd El-Naby H, Frisch W, Siebel W (2008) Tectono-metamorphic evolution of the Wadi Hafafit Culmination (central Eastern Desert, Egypt). Implication for Neoproterozoic core complex exhumation in NE Africa. Geol Acta 6:293–312

Abd El-Wahed M, Ashmawy M, Tawfik H (2010) Structural setting of Cretaceous pull-part basins and Miocene extensional folds in the Quseir-Umm Gheig region, northwestern Red Sea, Egypt. Lithosphere 2:13–32

Abdelsalam MG (1994) The Oko shear zone: post-accretionary deformations in the Arabian Nubian Shield. J Geol Soc London 151:767–776

Abdelsalam MG (2010) Quantifying 3D post-accretionary tectonic strain in the Arabian-Nubian Shield: superimposition of the Oko Shear Zone on the Nakasib Suture, Red Sea Hills, Sudan. J Afr Earth Sci 56:167–178

Abdelsalam MG, Stern RJ (1993) Tectonic evolution of the Nakasib suture, Red Sea Hills, Sudan: evidence for a late Precambrian Wilson cycle. J Geol Soc London 150:393–404

Abdelsalam MG, Stern RJ (1996) Sutures and shear zones in the Arabian-Nubian Shield. J Afr Earth Sci 23:289–310

Abdelsalam MG, Liégeois JP, Stern RJ (2002) The saharan metacraton. J Afr Earth Sci 34:119–136

Abu-Alam T, Stüwe K, Kadi K (2011) Pan-African exhumation mechanisms. Geophys Res Abstracts, EGU General Assembly 13: EGU2011-10307-1

Ali KA, Azer MK, Gahlan HA, Wilde SA, Samuel MD, Stern RJ (2010) Age constraints on the formation and emplacement of Neoproterozoic ophiolites along the Allaqi-Heiani Suture, Southeastern Desert of Egypt. Gondwana Res 18:583–595

Andresen A, Abu El-Rus MA, Myhre PI, Boghdady GY, Corfu F (2009) U-Pb TIMS age constraints on the evolution of the Neoproterozoic Meatiq Gneiss Dome, Eastern desert, Egypt. Int J Earth Sci 98(3):481–497. https://doi.org/10.1007/s00531-007-0276

Andresen A, Augland LE, Boghdady GY, Lundmark AM, Elnady OM, Hassan MA (2010) Structural constraints on the evolution of the Meatiq gneiss domes (Egypt), East-African Orogen. J Afr Earth Sci 57:413–422

Avigad D, Gvirtzman Z (2009) Late Neoproterozoic rise and fall of the northern Arabian-Nubian Shield: the role of lithospheric mantle delamination and subsequent thermal subsidence. Tectonophysics 477:217–228

Azer M, Stern RJ (2007) Neoproterozoic serpentinites in the Eastern Desert, Egypt: fragments of fore-arc mantle. J Geol 115:457–472

Bennett GD, Mosely P (1987) Tiered tectonics and evolution, Eastern Desert and Sinai, Egypt. In: Matheis G, Schandelmeier H (eds) Current research in African Earth sciences. Balkema, Rotterdam, The Netherlands, pp 79–82

Beyth M, Stern RJ, Matthews A (1977) Significance of high-grade metasediments from the Neoproterozoic basement of Eritrea. Precambrian Res 86:45–58

Bialas RW, Buck WR, Qin R (2010) How much magma is required to rift a continent? Earth Planet Sci Lett 292:68–78

Blank HR, Mooney WD, Healy JH, Gettings MA, Lamson RJ (1986) A seismic refraction interpretation of the eastern margin of the Red Sea depression, Southwest Saudi Arabia. US Geological Survey Open-file Report 86–257, 24 p

Blank HR, Johnson PR, Gettings ME, Simmons GC (1987) Geologic map of the Jizan quadrangle, Sheet 16F, Kingdom of Saudi Arabia. Saudi Arabian Directorate General of Mineral Resources Geoscience Map GM-104

Blasband B, White S, Brooijmans P, De Broorder H, Visser W (2000) Late Proterozoic extensional collapse in the Arabian-Nubian Shield. J Geol Soc London 157:615–628

Bohannon RG (1989) Style of extensional tectonism during rifting, Red Sea and Gulf of Aden. J Afr Earth Sci 8:589–602

Bonatti E (1985) Punctiform initiation of seafloor spreading in the Red Sea during transition from a continental to an oceanic rift. Nature 316:33–37

Bonatti E, Cipriani A, Lupi L (2015) The Red Sea: birth of an ocean. In: Rasul NMA, Stewart ICF (eds) The Red Sea: the formation, morphology, oceanography and environment of a young ocean basin. Springer Earth System Sciences, Berlin, pp 29–44. https://doi.org/10.1007/978-3-662-45201-1_2

Bosworth W (2015) Geological evolution of the Red Sea: historical background, review, and synthesis. In: Rasul NMA, Stewart ICF (eds) The Red Sea: the formation, morphology, oceanography and environment of a young ocean basin. Springer Earth System Sciences, Berlin, pp 45–78. https://doi.org/10.1007/978-3-662-45201-1_3

Bosworth W, Stockli DF (2016) Early magmatism in the greater Red Sea rift: timing and significance. Canadian J Earth Sci. https://doi.org/10.1139/cjes-2016-0019

Bosworth W, Huchon P, McClay K (2005) The Red Sea and Gulf of Aden basins. J Afr Earth Sci 43:334–378

Brueckner HK, Bonatti E, Elhaddad MA, Hamelin B, Kröner A, Reisberg L, Seyler M (1996) A Nd, Sr, Pb and Os study of the gneisses and ultramafic rocks of Zabargad Island, Red Sea: Miocene Moho or Pan African peridotites. J Geophys Res 100(B11):22283–22297

Burke K, Sengor C (1985) Tectonic escape in the evolution of the continental crust. In: Barazangi M, Brown L (eds) Reflection seismology: the continental crust. American geophysical union geodynamics series, vol 14, pp 41–53

Claesson S, Pallister JS, Tatsumoto M (1984) Samarium-neodymium data on two late Proterozoic ophiolites of Saudi Arabia and implications for crustal and mantle evolution. Contrib Mineral Petrol 85:244–252

Cochran JR (1983) A model for development of Red Sea. Bull Am Assoc Petrol Geol 67:41–69

Cochran JR, Martinez F (1988) Evidence from the northern Red Sea on the transition from continental to oceanic rifting. Tectonophysics 153:25–53

Coleman RG (1993) Geologic evolution of the Red Sea. Oxford Monographs on Geology and Geophysics. Oxford University Press, New York, 186 p

Coleman RG, Brown GF, Keith TEC (1972) Layered gabbros in southwest Saudi Arabia. U.S. Geological Survey Professional Paper 800-D:D143–D150

Coleman RG, Hadley DG, Fleck RJ, Hedge CT, Donato MM (1979) The Miocene Tihama Asir ophiolite and its bearing on the opening of the Red Sea. In: Al-Shanti AMS (ed) Evolution and mineralization of the Arabian-Nubian Shield. Pergamon Press, New York, pp 173–187

Collenette P, Grainger DJ (1994) Kyanite and andalusite. In: Collenette P, Grainger DJ (eds) Mineral resources of Saudi Arabia. Saudi Arabian Directorate General of Mineral Resources DGMR Special Publication SP2, pp 149–155

d'Almeida GAF (2010) Structural evolution history of the Red Sea rift. Geotectonics 44:271–282

DeMets C, Gordon RG, Argus DF (2010) Geologically current plate motions. Geophys J Int 181:1–80

DGMR (1977) Red Sea research 1970–1975. In: Saudi Arabian directorate general of mineral resources bulletin, vol 22, 223 p

Dixon TH, Ivins ER, Franklin BJ (1989) Topographic and volcanic asymmetry around the Red Sea: constraints on rift models. Tectonics 8:1193–1216

Drury SA, de Souza Filho CR (1988) Neoproterozoic terrane assemblages in Eritrea: review and prospects. J Afr Earth Sci 27:331–348

Duncan IJ, Rivard B, Arvidson RE, Sultan M (1990) Structural interpretation and tectonic evolution of the Najd Shear Zone (Saudi Arabia) using Landsat thematic-mapper data. Tectonophysics 178:309–315

El-Gaby S, List FK, Tehrani R (1988) Geology, evolution and metallogenesis of the Pan-African Belt in Egypt. In: El Gaby S, Greiling R (eds) The Pan-African Belt of NE Africa and adjacent areas, tectonic evolution and economic aspects. Vieweg, Braunschweig, Wiesbaden, pp 17–68

El-Gaby S, List FK, Tehrani R (1990) The basement complex of the Eastern Desert and Sinai. In: Said R (ed) The geology of Egypt. Balkema, Rotterdam, pp 175–184

Fritz H, Dallmeyer DR, Wallbrecher E, Loizenbauer J, Hoinkes G, Neumayr P, Khudeir AA (2002) Neoproterozoic tectonothermal evolution of the Central Eastern Desert, Egypt: a slow velocity tectonic process of core complex exhumation. J Afr Earth Sci 34:137–155

Fritz H, Abdelsalam M, Ali K, Bingen B, Collins AS, Fowler AR, Ghebreab W, Hauzenberger CA, Johnson P, Kusky T, Macey P, Muhongo S, Stern RJ, Viola G (2013) Orogen styles in the East African Orogens: a review of the Neoproterozoic to Cambrian tectonic evolution. J Afr Earth Sci 86:65–106

Gaina C, Gernigon L, Bail P (2009) Palaeocene-recent plate boundaries in the NE Atlantic and the formation of the Jan Mayen microcontinent. J Geol Soc London 66:606–616

Gettings ME, Blank HR, Mooney WD, Healey JH (1986) Crustal structure of southwestern Saudi Arabia. J Geophys Res 91:6491–6512

Ghebreab W, Talbot CJ, Page L (2005) Time constraints on exhumation of the East African Orogen from field observations and $^{40}Ar/^{39}Ar$ cooling ages of low-angle mylonites in Eritrea, NE Africa. Precamb Res 139:20–41

Gillman M (1968) Preliminary results of a geological and geophysical reconnaissance of the Jizan coastal plain in Saudi Arabia. In: AIME regional tech symposium rep 2d, Dhahran, pp 198–208

Girdler RW (1970) A review of Red Sea heat flow. Phil Trans R Soc Ser A 267:191–203

Girdler RW, Evans TR (1977) Red Sea heat flow. Geophys J R Astron Soc 51:245–252

Girdler RW, Styles P (1974) Two stage seafloor spreading. Nature 247:7–11

Golan, T, Katzir Y, Coble MA (2017) Early Carboniferous anorogenic magmatism in the Levant: implications for rifting in northern Gondwana. Int Geol Rev 60. https://doi.org/10.1080/00206814.2017.1326089

Goldberg M, Beyth M (1991) Tiran Island: an internal block at the junction of the Red Sea and Dead Sea transform. Tectonophysics 198:261–273

Greenwood WR, Anderson RE (1977) Palinspastic map of the Red Sea area prior to Miocene sea-floor spreading. In: Saudi Arabian directorate general of mineral resources bulletin, vol 22, pp Q1–Q6

Habib ME, Ahmed AA, El Nady OM (1985) Tectonic evolution of the Meatiq infrastructure, Central Eastern Desert, Egypt. Tectonics 4:613–627

Hall SA (1989) Magnetic evidence for the nature of the crust beneath the southern Red Sea. J Geophys Res 94:12267–12279

Hall SA, Andresen GE, Girdler RW (1977) Total-intensity magnetic anomaly map of the Red Sea and adjacent coastal area, a description and preliminary interpretation. In: Saudi Arabia directorate general of mineral resources bulletin, vol 22, pp F1–F13

Hamimi Z, El-Sawy EK, El-Fakharani A, Matsah M, Shujoon A, El-Shafei MK (2014) Neoproterozoic structural evolution of the NE-trending Ad-Damm Shear Zone, Arabian Shield, Saudi Arabia. J Afr Earth Sci 99:51–63

Handy MR, Brun J-P (2004) Seismicity, structure and strength of the continental lithosphere. Earth Planet Sci Lett 223:427–441

Hansen S, Schwartz S, Al-Amri A, Rodgers A (2006) Combined plate motion and density-driven flow in the asthenosphere beneath Saudi Arabia: evidence from shear-wave splitting and seismic anisotropy. Geology 34:869–872

Hansen SE, Rodgers AJ, Schwartz SY, Al-Amri AMS (2007) Imaging ruptured lithosphere beneath the Red Sea and Arabian Peninsula. Earth Planet Sci Lett 259:256–265

Hargrove US (2006) Crustal evolution of the Neoproterozoic Bi'r Umq suture zone, Kingdom of Saudi Arabia. Geochronological, isotopic, and geochemical constraints. Unpublished PhD thesis, University of Texas at Dallas, 343 p

Hosny A, Nyblade A (2016) Crustal structure of Egypt from Egyptian National Seismic Network data. Tectonophysics 687:257–267

Ilani S, Harlavan Y, Tarawneh K, Rabba I, Weinberger R, Ibrahim K, Peltz S, Steinitz G (2001) New K-Ar ages of basalts from the Harrat ash Shaam volcanic field in Jordan: implications for the span and duration of the upper-mantle upwelling beneath the western Arabian plate. Geology 29:171–174

Jackson J (2002) Strength of the continental lithosphere: time to abandon the jelly sandwich? GSA Today, September, pp 4–9

Japsen P, Chalmers JA, Green PF, Bonow JM (2011) Elevated, passive continental margins: not rift shoulders, but expressions of episodic, post-rift burial and exhumation. Glob Planet Change. https://doi.org/10.1016/j.gloplacha.2011.05.004

Johnson PR, Andersen A, Collins AS, Fowler AR, Fritz H, Ghebreab W, Kusky T, Stern RJ (2011) Late Cryogenian-Ediacaran history of the Arabian-Nubian Shield: a review of depositional, plutonic, structural, and tectonic events in the closing stages of the northern East African Orogen. J Afr Earth Sci 61:167–232

Kearey P, Klepeis KA, Vine FJ (2009) Global tectonics. Wiley-Blackwell, Chichester, UK, p 482

Kennedy A, Kozdroj W, Kattan FH, Kodzroj MZ, Johnson PR (2010) SHRIMP geochronology in the Arabian Shield (Midyan terrane, Afif terrane, Ad Dawadimi terrane) and Nubian Shield (Central Eastern Desert terrane) Part IV: data acquisition 2008. Saudi Geological Survey Open-File Report SGSOF-2010–10, 101 p

Khalil SM, McClay KR (2001) Tectonic evolution of the NW Red Sea-Gulf of Suez rift system. Geol Soc Spec Publ London 187:453–473

Khalil SM, McClay KR (2002) Extensional fault-related folding, northwestern Red Sea. Egypt. J Struc Geol 24:743–762

Kozdroj W, Kattan FH, Kadi KA, Al Alfy ZFA, Oweiss KA, Mansour MM (2011) SGS-EMRA Project for Trans-Red Sea Correlation between the Central Eastern Desert Terrane (Egypt) and Midyan Terrane (Saudi Arabia). Saudi Geological Survey Open-File Report SGS-TR-2011-5

Kusznir NJ, Park RG (1987) The extensional strength of continental lithosphere: its dependence on geothermal gradient and crustal thickness and composition. Geol Soc Spec Publ London 28:35–52

Lazar M, Ben-Avraham Z, Garfunkel Z (2012) The Red Sea—new insights from recent geophysical studies and the connection to the Dead Sea fault. J Afr Earth Sci 68:96–110

Levin V, Park J (2000) Shear zones in the Proterozoic lithosphere of the Arabian Shield and the nature of the Hales discontinuity. Tectonophysics 323:131–148

Ligi M, Bonatti E, Bortoluzzi G, Cipriani A, Cocchi L, Tontini FC, Carminati E, Ottolini L, Schettino A (2012) Birth of an ocean in the Red Sea: initial pangs. Geochem Geophys Geosyst 13. https://doi.org/10.1029/2012gc004155

Ligi M, Bonatti E, Rasul NMA (2015) Seafloor spreading initiation: geophysical and geochemical constraints from the Thetis and Nereus deeps, central Red Sea. In: Rasul NMA, Stewart ICF (eds) The Red Sea: the formation, morphology, oceanography and environment of a young ocean basin. Springer Earth System Sciences, Berlin, pp 79–98. https://doi.org/10.1007/978-3-662-45201-1_4

Manatschal G (2004) New models for evolution of magma-poor rifted margins based on a review of data and concepts from west Iberia and the Alps. Int J Earth Sci 93:432–466

Martinez F, Cochran JR (1988) Structure and tectonics of the northern Red Sea: catching a continental margin between rifting and drifting. Tectonophysics 150:1–31

McGuire AV, Coleman RG (1986) The Jabal Tirf layered gabbro and associated rocks of the Tihama Asir Complex, SW Saudi Arabia. J Geol 94:651–665

McKenzie D (1978) Some remarks on the development of sedimentary basins. Earth Planet Sci 40:25–32

Meinhold G, Morton AC, Avigad D (2013) New insights into peri-Gondwana paleogeography and the Gondwana super-fan system from detrital zircon U-Pb ages. Gondwana Res 23:661–665

Menzies MA, Klemperer SL, Ebinger CJ, Baker J (2002) Characteristics of volcanic rifted margins. Geol Soc Am Spec Paper 362:1–14

Meyer SE, Passchier C, Abu-Alam T, Stüwe K (2014) A strike-slip core complex from the Najd fault system, Arabian Shield. Terra Nova 26:387–394

Miller MM, Dixon TH (1992) Late Proterozoic evolution of the N part of the Hamisana zone, NE Sudan: constraints on Pan-African accretionary tectonics. J Geol Soc London 149:743–750

Mooney WD, Gettings ME, Blank HR, Healy JH (1985) Saudi Arabian seismic-refraction profile: a traveltime interpretation of crustal and upper mantle structure. Tectonophysics 111:173–246

Mutter JC, Talwani M, Stoffa PL (1982) Origin of seaward-dipping reflectors in oceanic crust off the Norwegian margin by "subaerial sea-floor spreading". Geology 10:353–357

Orszag-Sperber F, Harwood G, Kendall A, Purser BH (1998) A Review of the Evaporites of the Red Sea-Gulf of Suez rift. In: Purser BH, Bosence DWJ (eds) Sedimentation and Tectonics of Rift Basins: Red Sea-Gulf of Aden. Chapman and Hall, London, pp 409–426

Pallister JS (1986) Geologic map of the Al Lith Quadrangle, Sheet 20D, Kingdom of Saudi Arabia. Saudi Arabian Deputy Ministry for Mineral Resources Geoscience Map GM-95

Pallister JS (1987) Magmatic History of Red Sea rifting: perspectives from the central Saudi Arabian coastal plain. Geol Soc Am Bull 98:400–417

Pallister JS, Stacey JS, Fischer LB, Premo WR (1988) Precambrian ophiolites of Arabia: geologic settings, U-Pb geochronology, Pb-isotopes characteristics, and implications for continental accretion. Precamb Res 38:1–54

Pallister JS, McCausland WA, Jónsson S, Lu Z, Zahran HM, Hadidy SE, Aburukbah A, Stewart ICF, Lundgren PR, White RA, Moufti MRH (2010) Broad accommodation of rift-related extension recorded by dyke intrusion in Saudi Arabia. Nat Geosci 3:705–712

Park Y, Nyblade AA, Rodgers AJ, Al-Amri A (2008) S wave velocity structure of the Arabian Shield upper mantle from Rayleigh wave tomography. Geochem Geophys Geosyst 9. https://doi.org/10.1029/2007gc001895

Pearce JA, Bender JF, De Long SE, Kidd WSF, Low PJ, Güner Y, Saroğlu R, Yilmaz Y, Moorbath S, Mitchell JG (1990) Genesis of collision volcanism in Eastern Anatolia, Turkey. J Volcan Geotherm Res 44:189–229

Powell JH, Abed AM, Le Nindre Y-M (2014) Cambrian stratigraphy of Jordan. GeoArabia 19:81–134

Prodehl C (1985) Interpretation of a seismic-refraction survey across the Arabian shield in western Saudi Arabia. Tectonophysics 111:247–282

Rasul NMA, Stewart ICF (2015) The Red Sea: the formation, morphology, oceanography and environment of a young ocean basin. Springer Earth System Sciences, Berlin, 638 p

Rasul NMA, Stewart ICF, Nawab ZA (2015) Introduction to the Red Sea: its origin, structure, and environment. In: Rasul NMA, Stewart ICF (eds) The Red Sea: the formation, morphology, oceanography and environment of a young ocean basin. Springer Earth System Sciences, Berlin, pp 1–28. https://doi.org/10.1007/978-3-662-45201-1_1

Reilinger R, McClusky S, Ar Rajehi A (2015) Geodetic constraints on the geodynamic evolution of the Red Sea. In: Rasul NMA, Stewart ICF (eds) The Red Sea: the formation, morphology, oceanography and environment of a young ocean basin. Springer Earth System Sciences, Berlin, pp 135–149

Roeser HA (1975) A detailed magnetic survey of the southern Red Sea. Geol Jahrb D13:131–153

Roobol MJ, Stewart ICF (2009) Cenozoic faults and recent seismicity in northwest Saudi Arabia and the Gulf of Aqaba region. Saudi geological survey technical report SGS-TR-2008-7, 35 p

Saleh S, Jahr T, Jentzsch G, Saleh A, Abou Ashour NM (2006) Crustal evaluation of the northern Red Sea rift and Gulf of Suez, Egypt from geophysical data: 3-dimensional modeling. J Afr Earth Sci 45:257–278

Schardt C (2016) Hydrothermal fluid migration and brine pool formation in the Red Sea: the Atlantis II Deep. Miner Deposita 51:89–111

Sebai A, Zumbo V, Férand G, Bertrand H, Hussain AG, Giannérini G, Campredon R (1991) 40Ar/39Ar dating of alkaline and tholeiitic magmatism of Saudi Arabia related to the early Red Sea rifting. Earth Planet Sci Lett 104:473–487r

Shimron AE (1989) The Red Sea Line—a Late Proterozoic transcurrent fault. J Afr Earth Sci 11:95–112

Squire RJ, Campbell IH, Allen CM, Wilson CJL (2006) Did the Transgondwanan Supermountain trigger the explosive radiation of animals on Earth? Earth Planet Sci Lett 250:116–133

Stern RJ (1985) The Najd Fault System, Saudi Arabia and Egypt: a late Precambrian rift-related transform system. Tectonics 4:497–511

Stern RJ (1994) Neoproterozoic (900-550 Ma) arc assembly and continental collision in the East African Orogen. Ann Rev Earth Planet Sci 22:319–351

Stern RJ (2002) Crustal evolution in the East African Orogen: a neodymium isotopic perspective. J Afr Earth Sci 34:109–117

Stern RJ (2017) Neoproterozoic formation and evolution of Eastern Desert continental crust—the importance of the infrastructure-superstructure transition. J African Earth Sci. https://doi.org/10.1016/jafreasci.2017.01.001

Stern RJ, Johnson PR (2010) Continental lithosphere of the Arabian Plate: a geologic, petrologic, and geophysical synthesis. Earth-Sci Rev 101:29–67

Stern RJ, Kröner A, Manton WI, Reischmann T, Mansour MM, Hussein IM (1989a) Geochronology of the late Precambrian Hamisana shear zone, Red Sea Hills, Sudan and Egypt. J Geol Soc London 145:1017–1029

Stern RJ, Kröner A, Manton WI, Reischmann T, Mansour M, Hussein IM (1989b) Geochronology of the late Precambrian Hamisana shear zone, Red Sea Hills, Sudan and Egypt. J Geol Soc London 146:1017–1029

Stern RJ, Nielsen KC, Best E, Sultan M, Arvidson RE, Kröner A (1990) Orientation of late Precambrian sutures in the Arabian Nubian shield. Geology 18:1103–1106

Stern RJ, Johnson PJ, Kröner A, Yibas B (2004) Neoproterozoic ophiolites of the Arabian-Nubian Shield. In: Kusky T (ed) Precambrian Ophiolites. Elsevier, pp 95–128

Stern RJ, Ren M, Ali K, Förster H-J, Al Safarjalani A, Nasir S, Whitehouse MJ, Leybourne MI (2014) Early Carboniferous (~357 Ma) crust beneath northern Arabia: tales from Tell Thannoun (southern Syria). Earth Planet Sci Lett 393:83–93

Stern RJ, Ali KA, Ren M, Jarrar GH, Romer RL, Leybourne MI, Whitehouse MJ, Ibrahim KM (2016) Cadomian (~ 560 Ma) crust buried beneath the northern Arabian Peninsula: mineral, chemical, geochronological, and isotopic constraints from NE Jordan xenoliths. Earth Planet Sci Lett 436:31–42

Stewart ICF, Johnson PR (1994) Satellite gravity and Red Sea tectonics. Saudi Arabian Deputy Ministry for Mineral Resources Open-File Report USGS-OF-94-10, 22 p

Stoeser DB, Frost CD (2006) Nd, Pb, Sr, and O isotopic characterization of Saudi Arabian Shield terranes. Chem Geol 226:163–188

Suayah IB, Rogers JJW, Dabbagh ME (1991) High-Ti continental tholeiites from the Aznam trough, northwestern Saudi Arabia: evidence of "abortive" rifting in the "embryonic" stage of Red Sea opening. Tectonophysics 191:75–87

Sultan M, Arvidson RE, Duncan IJ, Stern RJ, El Kaliouby B (1988) Extension of the Najd shear system from Saudi Arabia to the Central Eastern Desert of Egypt based on integrated field and Landsat observations. Tectonics 7:1291–1306

Sultan M, Becker M, Arvidson RE, Shore P, Stern RJ, El Alfy Z, Attia RI (1993) New constraints on Red Sea rifting from correlations of Arabian and Nubian Neoproterozoic outcrops. Tectonics 12:1303–1319

Szymanski E (2013) Timing, kinematics, and spatial distribution of Miocene extension in the central Arabian margin of the Red Sea rift system. PhD dissertation, U Kansas, 430 p

Szymanski E, Stockli DF, Johnson PR (2012) Evidence for an early and sustained mode of diffuse lithospheric extension in the central Arabian flank of the Red Sea rift system: implications for margin structural; kinematics and basin development. In: The American association of petroleum geologists annual convention and exhibition, Long Beach, CA, abstract no. 1235423

Szymanski E, Stockli DF, Johnson PR, Hager C (2016) Thermochronometric evidence for diffuse extension and two-phase rifting within the central Arabian margin of the Red Sea Rift. Tectonics 35. https://doi.org/10.1002/2016tc004336

Szymanski E, Stockli DF, Johnson PR, Kattan FH, Al Shammari A (2007) Observations from fieldwork and (U-Th)/He thermochronologic study of the central Arabian flank of the Red Sea rift system. In: The American geophysical union, fall meeting 2007, abstract #T41A-0379

Tang Z, Julià J, Zahran H, Mai PM (2016) The lithospheric shear-wave velocity structure of Saudi Arabia: young volcanism in an old shield. Tectonophysics 680:8–27

Thomas WA (2006) Tectonic inheritance at a continental margin. GSA Today 16(2):4–11. https://doi.org/10.1130/1052-5173(2006)016%3c4:TIAACM%3e2.0.CO;2

Vail JR (1985) Pan-African (Late Precambrian) tectonic terranes and the reconstruction of the Arabian-Nubian shield. Geology 13:839

Voss M, Jokat W (2007) Continent-ocean transition and voluminous magmatic underplating derived from P-wave velocity modeling of the East Greenland continental margin. Geophys Res Lett 170: 580–604

Wegener A (1920) Die Entstehung der Kontinente und Ozeane. Vieweg, Brunswick, p 135

Wolfenden E, Ebinger C, Yirgu G, Renne P, Kelley S (2005) Evolution of a volcanic rifted margin: Southern Red Sea, Ethiopia. Geol Soc Am Bull 117:846–864

Zahran HM, Stewart ICF, Johnson PR, Basahel MH (2003) Aeromagnetic anomaly maps of central and western Saudi Arabia. Saudi Geological Survey Open-File Report SGS-OF-2002-8